FINAL REPORT

STUDIES RELEVANT TO THE ELECTRIC VACUUM GYRO PROGRAM OF ELECTRICAL BREAKDOWN IN ULTRAHIGH VACUUM

Ernest M. Lyman

REPORT R-334 JANUARY, 1967

This work was supported in part by the Joint Services Electronics Program (U.S. Army, U.S. Navy, and U.S. Air Force) under Contract DA 28 043 AMC 00073(E); and in part by the NASA NGR 14 005 038.

This is the final report, submitted in fulfillment of the requirements of NASA Grant NGR 005 038 (terminated on 30 September 1966) and the Joint Services Electronics Program (U. S. Army, U. S. Navy, and U. S. Air Force) under Contract No. DA 28 043 AMC 00073(E).

Matters concerned with various aspects of the electrostatically levitated gyroscope have previously been reported in detail.[1] The recent activities reported here have been concerned with a study of the nature of electrical breakdown in ultrahigh vacuum, and some measurements directly related to the gyro development.

The following tasks were performed during the period:

1. Experimental measurements were made on the effect of gas-conditioning in suppressing field emission current and improving the voltage holding capabilities of plane tungsten electrodes in ultrahigh vacuum. By gas-conditioning the electrodes, an improvement in the breakdown voltage by a factor of 3 to 4 was achieved. A quantitative explanation of the effect, in agreement with experiment, was developed. The theory and experimental results were reported at the Second International Symposium on Insulation of High Voltages in Vacuum held at MIT on 7 September 1966 and are printed in the Proceedings of that meeting.[2] A short version of the report[3] will appear as a Communication in the Journal of Applied Physics early in 1967. This work is described in Appendix A.

2. Apparatus was constructed and experimental work started on the study of the work function of portions of a tungsten emitter tip exhibiting the "flicker effect" in field emission. This effect may be related to the

process of formation of whiskers or protuberances on the electrodes in high vacuum. Several observations were made on the effect, but due to the lack of time, no quantitative measurements were obtained. The progress of this activity is outlined in Appendix B.

3. The present picture of the initiating mechanism of electrical breakdown in ultrahigh vacuum is based upon the observed fact that metallic protuberances exist on the cathode. Two types of experiments were performed to attempt to discover the mechanism of formation of these protuberances or whiskers. If whiskers could be prevented from re-forming they could be eliminated by the gas-conditioning described above and breakdown voltages could be raised by one to two orders of magnitude. In Appendix C, the studies using a field emission microscope tube are described, while in Appendix D, the studies using electrodes inside a shadow electron microscope are discussed.

Whiskers have been seen to appear and disappear in both studies, but contrary to our previous observations they were not found to be produced when the electrodes were operated in the "unstable current mode." This work is continuing in order to resolve the contradiction, with emphasis at the moment on the electron microscope method.

4. A technological investigation was made of the effects on the voltage-current characteristics of a teflon pad cemented to the molybdenum electrode of a molybdenum-beryllium pair of plane electrodes. The purpose of the teflon is to prevent scuffing of the gyro ball if it is dropped onto the electrodes while spinning. A qualified conclusion of these

measurements is that under certain conditions the teflon button has no significant effect upon these characteristics. See Appendix E.

5. A major effort went into developing physical explanations of various aspects of the electrical breakdown problem. In addition to the papers mentioned above, the following papers were written and are appended in Appendix F.

a) "Field Emission from a Multiplicity of Emitters on a Broad Area Cathode," by H. E. Tomaschke and D. Alpert, to appear as a Communication in the Journal of Applied Physics early in 1967.

b) "The Role of Submicroscopic Projections in Electrical Breakdown," by H. E. Tomaschke and D. Alpert, completed in final form to be submitted to the Journal of Vacuum Science and Technology.

The following review paper was presented by D. Alpert at the 26th Annual Conference on Physical Electronics at MIT on March 22, 1966: "Electrical Breakdown in Ultrahigh Vacuum."

APPENDIX A

The Effect of Gas Pressure on Electrical Breakdown and Field Emission

by

E. M. Lyman, D. A. Lee, H. E. Tomaschke and D. Alpert

One of the significant consequences of the physical picture for the initiation of electrical breakdown between metallic electrodes in ultrahigh vacuum, as previously reported,[4] has been the development of a physical explanation for the so-called "gas effect" which has often been noted but heretofore not understood. Several authors[5,6,7] have noted that when a gas was introduced into the vacuum system to a pressure of about 10^{-4} Torr, the predischarge currents were typically reduced and the breakdown properties improved. The observed effects were not strongly dependent upon the nature of the gas; in particular, no significant differences were noted as between noble and molecular gases of comparable mass. We have observed similar effects when gas is admitted to systems containing clean tungsten electrodes.

Since the gap spacings in most of the above experiments were smaller than the mean free path for atomic collisions, the "gas effect" could not readily be attributed to interactions in the volume; yet an effect sensitive to the pressure, but not to the chemical nature of the gas, seemed to be equally difficult to ascribe to atomic interactions at the electrode surfaces.

To explain this so-called "gas effect," we assume as a starting point the breakdown model[4] based on field emission from submicroscopic projections. When gas is introduced, the significant decrease in field emission is here attributed to the selective sputtering of the emitting whiskers by ions formed in the volume by electron bombardment of the gas molecules. If the ions were created uniformly in the gap volume, the probability of striking a given projection would be very small indeed, since the cross-sectional area of an individual emitter lies in the range of 10^{-12} to 10^{-10} cm^2. However, as is suggested by the schematic representation in Fig. 1, the formation of ions by impinging electrons is not uniformly distributed; on the contrary, it is restricted to localized regions adjacent to the emission sites. Hence, these ions have a much higher probability of striking the corresponding emitting projection, and they do so with sufficient energy to cause sputtering and thus a change in geometrical shape.

In view of the complex dependence of the probability of ionization on the energy of colliding electrons, it is not easy to make an accurate calculation of the number and distribution of the ions formed in the volume. However, it is possible to make certain order-of-magnitude estimates which provide quantitative support and added plausibility for the above picture. Consider the following hypothetical situation, which is derived from a rather typical experimental observation (with tungsten electrodes). For a broad area configuration with electrodes of about 3 cm diameter and 1 mm gap spacing, the breakdown voltage is approximately 60 kV, while the total current just prior to breakdown is of the order of 200 μA. Let us consider the ion production at some value below breakdown, say at an applied voltage,

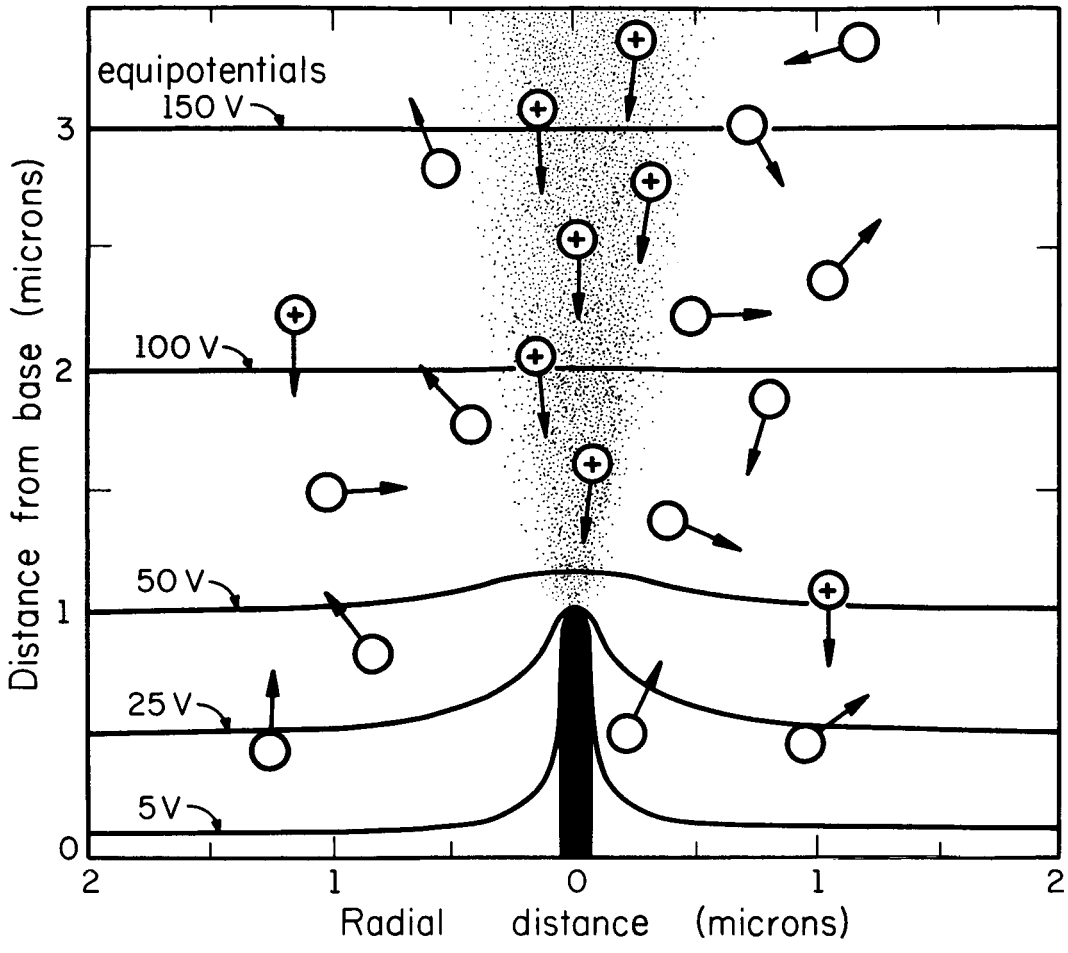

Figure 1.

Schematic representation of selective ion bombardment of a one-micron (10^{-4} cm) projection. Calculated equipotentials are shown for an average electric field of 5×10^5 volts/cm.

V_A, of 48 kV where the emission current is about 10 μA. At a pressure (for nitrogen) of 10^{-4} Torr, the overall probability of forming ions in the volume by electron collision is estimated to be approximately 10^{-5} ions per electron for the above gap spacing. This assumes an average ionization efficiency of about 10% of the maximum value, which is approximately 10 ions/electron/cm path length/Torr, for an electron energy of 100-200 eV. (The efficiency drops off considerably for higher energies.) If the resulting ion current, 10^{-10}A were uniformly distributed over the entire cathode area, the number of ions striking unit area per second under these conditions would be about 10^8 ions/cm^2/sec. This corresponds to the deposition of a monolayer of ionized gas in 10^7 seconds, i.e., in the order of months, and would not result in rapid sputtering of the emitter tips.

The shape of a typical emitting whisker can be approximated by a prolate spheroid, as shown in Figure 1, roughly 10^{-4} cm in height and 10^{-5} cm in base diameter. Typically, the emitting area is some small fraction (a few percent) of the base area, and, for the dimensions shown, the localized enhancement of the electric field at the tip is approximately 100. Hence, even allowing for the spreading due to space charge,[8] the electrons traverse the gap in narrow pencil-like beams, originating only at the sharpest projections. Furthermore, the highest probability for ion production lies in the portion of the electron trajectory in which its energy is of the order of 100 eV, i.e., in the cylindrical microvolume immediately above the whisker and roughly of the same dimensions, as shown schematically in Figure 1.

When the applied voltage is 80% of the breakdown value, the local field at the emitter tip is approximately 5×10^{7} V/cm, while the average electric field within the gap (for an enhancement factor of 100) is about 5×10^{5} V/cm. As indicated by the calculated equipotentials superimposed in Figure 1, the energy of the electrons impinging on the neutral gas molecules ranges from 50 eV at a distance of 1.8×10^{-5} cm to 100 eV at 10^{-4} cm above the emitter tip. Corresponding energies are transferred to the ions when they impinge on the emitter surface. A crude calculation indicates that under these conditions of field and gas pressure, the current density is sufficient (8×10^{5}A/cms^{2}) that a sizeable fraction (several percent) of the neutral gas molecules entering the microvolume are ionized. In view of their proximity, a large fraction of these will strike the projection; the resulting rate of arrival of energetic ions at the emitting tip corresponds to tens of monolayers of gaseous ions per second at a pressure of 10^{-4} Torr.

Since energies of 50 to 100 eV are quite sufficient to cause sputtering or similar dislocation damage to the emitting whisker, this effect can readily explain a significant change in its shape. Assuming a typical sputtering efficiency of a few percent, a measurable change might be expected within minutes. It is estimated that the most rapid change in enhancement factor, β, under the above conditions occurs for projections about one-micron high. For smaller projections, the sputtering ions are not so strongly focused on the tip since they are created far from it; hence, β changes more slowly because the sputtering rate is low. For larger projections, since the fractional rate of removal of material is roughly inversely proportional to the linear dimensions, the rate of

change of β is also less than for the one-micron whiskers. The exact rate of change of the enhancement factor would therefore depend on the size and shape of the projection, the gas and its pressure, the ionization probability, and the sputtering rates for the ions and electrode material in question.

Two experiments of a preliminary nature have been carried out to test the qualitative conclusions presented above. In the first, a small tungsten electrode was inserted into a modified field-emission microscope,[9] and the applied voltage adjusted to give a field-emission current of 10^{-6}A. With the voltage off, argon gas was admitted to a pressure of about 3×10^{-5} Torr. The voltage was then raised to the value at which the current reached its former value of 10^{-6}A. With the voltage held constant at this value, the current was observed to rise rapidly to a maximum value of about 10^{-5}A (in a matter of a minute or less) and then to decrease more gradually to a new equilibrium value of 2 or 3×10^{-7}A. The time elapsed for the entire process was of the order of a few minutes. If the voltage was thereupon increased, the process would repeat, although the magnitudes of the current and time interval might vary, depending on the previous treatment of the cathode.

It seems reasonable to postulate that the initial increase in current is due to a sharpening of the whisker by the initial sputtering at glancing angles; the subsequent decrease in current is attributed to a more gradual dulling process as the tip of the projection is eroded away. Although changes in the work function of the emitting projection might

also account for the changes in the emission current, the lack of sensitivity of the effect to the chemical nature of the gas suggests that this is not the dominant process.

In the second set of experiments the apparatus included the 3.5-cm diameter flat electrodes cut from a single-crystal tungsten boule and mechanically and electrically polished, as described.[4] After bakeout at 450°C and repeated breakdown runs in ultrahigh vacuum, the breakdown voltage approached a reproducible value of 36 kV $\pm$ 10% at a gap spacing of 0.71 mm. Thus, at breakdown, the average field, F_o, in the gap was 5.1×10^5 V/cm $\pm$ 10%. The emission current just below the breakdown point was 100 μA. The enhancement factor, β, as deduced from the Fowler-Nordheim plots was also fairly reproducible at $\beta = 126 \pm 10\%$ and the critical field $F_{crit} = \beta F_o$ at the emitter tips at breakdown was 6.4×10^7 V/cm, in substantial agreement with earlier results.

Argon gas was then introduced into the system to a pressure of 10^{-4} Torr while the voltage was held at 28 kV. The initial current of 5 μA increased immediately to 10 μA, then fell slowly over a period of several hours to 0.5 μA. The x-ray yield was at all times proportional to the current, showing that the current was mainly due to electrons having the full gap energy. Additional gas treatments, totaling about 15 hours, further suppressed the current to about ½% of its original value, where it remained, or decreased slightly when the system was evacuated. The enhancement factor of the conditioned surface was measured to be 90, with a corresponding increase in breakdown voltage to 41 kV.

In a second type of experiment with the broad-area electrodes, after admitting gas at 10^{-4} Torr, the current was held constant at 100 to

Table I. Vacuum Insulation Properties of Flat Tungsten Electrodes 3.5 cm in Diameter

	V_{BD}(kV)	β	$F_{crit}(\frac{MV}{cm})$	$F_o(\frac{MV}{cm})$	area(cm^2)
A. Gap = 0.71 mm					
1. New, baked out	36	126	64	0.51	7.6×10^{-11}
2. After low-current gas conditioning	41	90	52	0.58	
3. After outgassing anode	59	71	59	0.83	8.1×10^{-12}
4. After anode outgas and gas conditioning	116	26	43	1.63	1.6×10^{-9}
5. Ratio: $\frac{\text{Row 4}}{\text{Row 1}}$	3.2	1/4.8	1/1.5	3.2	21.
B. Gap = 0.25 mm					
6. New, baked out	13	94	49	0.52	5.2×10^{-12}
7. After gas conditioning	22	60	53	0.88	2.9×10^{-10}
8. After gas conditioning anode at LN temp.	33	36	47	1.32	7.2×10^{-10}
9. After anode outgas and gas conditioning	52	19	40	2.08	3.5×10^{-9}
10. Ratio: $\frac{\text{Row 9}}{\text{Row 6}}$	4.0	1/4.9	1/1.2	4.0	67.

300 μA by continuously adjusting the voltage upward as surface conditioning proceeded. In one run, the enhancement factor was lowered to 26 with an accompanying increase in the breakdown voltage to 116 kV, corresponding to an average field in the gap of $F_o = 1.6 \times 10^6$ V/cm at breakdown. It should be remarked that the volt-ampere characteristic from which β is deduced cannot be measured with gas present because the surface changes occurring during the measurement render the data unreproducible.

The observed vacuum-insulation properties of the electrodes at gap spacings of 0.71 mm and 0.25 mm at various stages of the gas conditioning are illustrated in Table I.

From the table it can be seen that the combination of selective sputtering and anode outgassing may decrease the enhancement, β, by a factor of about 4 with a corresponding increase of the voltage-holding capabilities by a factor of 3 to 4. In one run at 0.25-mm gap, a value of $\beta = 14.5$ was achieved with a breakdown voltage of 81 kV corresponding to an average field in the gap of over 3×10^6 V/cm.

The emitting area increases greatly as the sharp tips are blunted during selective sputtering. Consequently, the predischarge emission current near breakdown for the conditioned electrodes may be from one to two orders or magnitude higher than for the fresh electrodes. As a practical matter in vacuum insulation, anode heating and x-radiation may become a more serious problem because of the combination of high voltage and high current. On the other hand, even taking into account the increase in area, a reduction in enhancement factor from 100 to 20 should, on theoretical grounds, be accompanied by a reduction in field-emission current by almost 20 orders of magnitude. Experimentally, for the 0.25-mm gap with 81-kV

breakdown voltage, the current dropped to our lowest measurable value (10^{-10}A) at an applied voltage of 42 kV corresponding to an average field in the gap of 1.7×10^{6} V/cm.

Estimates of the time constants for blunting of the new sharp whiskers formed during a spark were made by observing the fading of the transition radiation that appears on the anode opposite a new emitter point. At 10^{-4} Torr and 1 mA emission current, the fading of a sharp blue spot into the general blue background (due to many weaker emitters) occurred in a few seconds. At 10^{-5} Torr, the time constant was of the order of tens of seconds except for giant emitters which heated the anode spot white hot. As predicted above, these large protrusions were not noticeably affected by the sputtering and could only be burned off with great difficulty at high currents (5 mA). After blunting of the sharpest whiskers, the rate of decrease of enhancement factor is small. Conditioning to the point indicated in Row 9 of the table required about 20 hours.

These results differ in one important way from those of earlier workers who reported that the voltage holding properties returned to their original characteristics (breakdown voltage) almost immediately after the gas was removed and the system evacuated. Preliminary observations on this system (at 3×10^{-10} Torr) indicate a time of the order of a week or two for the increase of β by a factor of two. It can only be conjectured here that the surface contamination in these earlier experiments may have contributed to the redevelopment of sizeable protuberances as soon as the selective sputtering process was terminated or that the conduction and its suppression were associated with inherently different physical mechanisms.

It may also be conjectured that the final values of breakdown parameters reached in our experiments represent an equilibrium between blunting and regeneration of protrusions on the cathode.

Our detailed experiments have thus far been carried out only with tungsten electrodes. It will be of considerable interest to continue these studies with other materials as well, to determine the effects of selective ion bombardment and the rate of formation of new whiskers after the gas is removed.

APPENDIX B

Flicker Effect

The object of this work was to study the so-called flicker effect in field emission which may be postulated to be due to the adsorption and desorption of gas molecules at emission sites. The interesting characteristic of the effect is the rigorously bistable nature of the current from the flickering spot on the field-emission pattern of an emitting tip. By obtaining Fowler-Nordheim plots of the current-voltage characteristics of the spots in the "on" and "off" modes, one might hope to provide some quantitative clues as to the physical phenomenon involved.

A simplified version of the Young-Müller[10] apparatus was constructed in which a small portion of the emission pattern from the cathode tip was passed through a small hole in the anode and the current was collected in a Faraday cup. Two versions of the apparatus were constructed. In the first, the portion of the emission pattern striking the anode hole was selected by magnetic deflection, which, due to the nature of the

design, interacted with the accelerating voltage and gave non-linear Fowler-Nordheim plots. In the second, the tip and an anode ring were mechanically rotated to admit the desired portion to the cup.

The operation of the second version appears to be satisfactory but no data have been obtained with it. The experiment will be resumed at a later date.

APPENDIX C

Field-Emission Study of Whisker Production

In previous work[11] with closely-spaced, small electrodes it was found that under certain conditions, namely with a gas-covered anode, numerous, fine, whisker-like projections could be produced on the emitter. (These whiskers were observed with an electron microscope.) The production of these whiskers was associated with an "unstable" behavior of the emission characteristics in which large current fluctuations were observed. It was decided to continue this study using field-emission techniques. The procedure used was as follows: First the emission pattern from an emitter was viewed on a screen. Next, an anode was interposed between the emitter and screen and was positioned at a small distance from the emitter. This anode was purposely not outgassed so that ions produced at its surface could bombard the emitter surface and, in theory, produce sites for whisker growth. The third step was to swing the anode out of the way and again view the emission pattern on the screen. The presence of whiskers would be expected to produce a number of new spots of illumination on the screen.

The experimental apparatus included a phosphor-coated disk mounted on a press at one end of the cylindrical bell jar. From the same press, support wires projected out past the disk into the bell jar. An emitter which faced the disk was mounted on these support wires. The emitter consisted of the blunt end of a 3-mil tungsten wire spotwelded to a 10-mil tungsten filament. A press mounted on a metal bellows was attached to the other end of the bell jar. A loop of 10-mil tungsten wire serving as the anode was spotwelded to the support wires from this second press. This loop could be interposed between the emitter and the disk.

Although the data obtained from this apparatus are relatively meager, the results have all been negative. That is, after placing the anode next to the emitter and operating in the "unstable" mode, i.e., with large current fluctuations, for periods as long as one hour, there were no indications in the emission pattern that whiskers had been produced on the emitter.

In continuing this study, it now seems necessary to look carefully for differences in the present procedure as compared with that used previously (in the electron-microscope case) in which fine whiskers were observed. One obvious difference is that in the previous case the cathode was alternately subjected to ion bombardment in an ultrahigh vacuum and then subjected to electron bombardment in an oil-contaminated system.

APPENDIX D

Electron-Microscope Study of Whisker Production

In addition to the search for whisker production using the field-emission microscope as the detector, a search using an RCA Electron Diffraction Unit (a prototype of the Type EMD) in the shadow electron-microscope mode of operation has been started. Electrodes have been mounted in the specimen chamber. The blunt end of a 3-mil tungsten wire has been used as the cathode electrode. This electrode is mounted on a 10-mil tungsten loop for heating purposes. The electropolished end of a 100-mil tungsten rod has served as the anode. The gap spacing has been about 5 mils.

Changes in the cathode profile due to electrical breakdown have been observed. Both the destruction and the formation of projections have been noted.

Attempts to measure field-emission currents in order to plot F-N curves have been unsuccessful due to the large current fluctuations. Some reduction in fluctuation has been obtained by operating the cathode at elevated temperatures. Presumably this reduces the amount of contamination on the cathode.

Preliminary attempts to produce whiskers by operating in the "unstable" mode have given negative results. However, because of the poor vacuum conditions it is questionable whether or not the observed current fluctuations are due to the same conditions as those which were present in the ultrahigh vacuum system in which the "unstable" mode was originally observed.

APPENDIX E

Technological Measurements of the Current-Voltage Characteristics of a Pair of Be - Mo Electrodes in High Vacuum

by

W. Schuemann, W. Anderson and E. M. Lyman

The purpose of this experiment was (1) to measure the volt-ampere characteristics of a pair of flat disks, one of beryllium and the other of molybdenum, used as electrodes in high vacuum, simulating conditions in the electrostatically supported gyroscope and (2) to compare them with the characteristics of another pair of electrodes similar except for a teflon pad cemented to the molybdenum disk. The purpose of the pad is to prevent scuffing of the gyro ball in the starting and stopping procedures.

I. General Procedure

A set of plain one-inch diameter disk-shaped Mo - Be electrodes was installed in a vacuum bell jar, baked out at 100°C, spaced to a 0.002-inch gap and electrically conditioned by raising the voltage slowly to prevent excessive sparking until an emission current of 50 μA was obtained (at currents appreciably higher than this, continuous sparking occurred). After several hours of conditioning at 50 μA, during which the sparking rate gradually dropped to less than one spark per minute, current-voltage characteristics of the electrode pair were measured. Fowler-Nordheim (see section III) plots of the data (measured over currents, in some instances, ranging from 50 μA to 0.05 μA) could be interpreted as straight lines

suggesting that the electrode current was entirely due to field emission. As shown in Table II, values of the field enhancement factor β obtained from the F-N plots typically range from 170 to 390. In calculating β it was assumed that the appropriate work function to be used was that of the cathode material, in each case.

Similar measurements were made on a Be - Mo pair of electrodes which had a teflon disk 5/16-inch in diameter 0.0005-inch thick cemented to the center of the molybdenum disk. As shown in Table II, the calculated β's range from 105 to 340.

Details of the runs in which four sets of disks were used are given in section III with descriptions of the physical appearance of the electrodes after removal from the bell jar.

II. Discussion of Results

1. Plain electrodes (Sets I and III)

For each set of electrodes the average value of β obtained when molybdenum was cathode is higher than when beryllium was cathode. For set I the ratio of the β's is 1.14; in set III, it is 1.21. As shown in the section III the ratio of $(\phi^{3/2})$ used to calculate the β's is 1.11. Within the precision of the experiment all of these ratios are equal. It is well known that electrode material is transferred during sparking, and this suggests that during the conditioning, sufficient Be (m.p. 1278^{o}C) was transferred to the Mo (m.p. 2620^{o}C) to give both surfaces the characteristics of the Be. If both surfaces are the same, the average electrode voltage for 50 μA might also be expected to be independent of polarity. This is the case in set I, but not in set III.

If it is assumed that the electrode voltage at 50 μA current is the breakdown voltage, the initial field at the cathode emitter tips for both sets I and III is about 1.1×10^8 volts/cm, a value in substantial agreement with previous observations on a variety of other metals.[12,13,14]

Thus the behavior of the plain Be - Mo electrodes with respect to the volt-ampere characteristics and the critical field required for breakdown is in accord with the current picture of initiation of vacuum breakdown based on Joule-heating, melting and vaporization of whiskers on the cathode surface.

2. Electrodes with a teflon pad on the Mo disk (Sets II and IV)

As in the case of the plain electrodes the value of β obtained when Mo was the cathode material are consistently higher than when Be was the cathode material. In set II, the ratio of the average values of β is 2.48, while for set IV it is 1.53. Both of these ratios are too high to be explained on the basis of the ratio of $(\phi^{3/2})$ of the cathode metals. The inconsistent results of sets II and IV, both electrical, and also as regards physical appearance after the tests, see section III, prevents qualitative or quantitative physical interpretation of the phenomena. In comparing electrode pairs with and without the teflon disks, in one case (set II) one might conclude that the teflon disk had little effect on the volt-ampere characteristics or the breakdown voltage V_{max}, while in the other (set IV) the breakdown voltage was only half as much as for plain electrodes, due, possibly, to the carbonization of the teflon which would be expected to have a pronounced effect upon the effective work functions and upon the effective gap spacing.

III. Apparatus and Detailed Experimental Procedure

Apparatus: Schematic circuits and apparatus diagrams are shown in Figure 2.

The electrodes were washed and installed in the chamber. One electrode was fixed, while the other was on a rotating ball-and-socket type mount to insure the electrodes being parallel. The chamber was sealed using gold O-rings. The electrodes were zeroed using an ohm-meter to determine the point of contact. Next, the system was roughed with the roughing pump and the Zeolite. The Zeolite was baked out overnight at 200°C, then cooled with liquid nitrogen for about 2 hours to rough the system. The vac-ion pump was then started, and the electrodes and vac-ion pump were baked out for 2 to 3 days at 100°C. The gap was left at 20 mils for bakeout. After bakeout, the gap was set at 2 mils for data-taking.

Set I: Be-Mo

The Be was first used as the anode, the Mo as the cathode. The current into the electrodes was raised from 10 μA to 50 μA in steps of 5 or 10 μA, remaining for a few minutes at each setting. The time, pressure, electrode voltage, and breakdown activity were recorded at each setting. Before going on to each new value of current, the breakdown rate was allowed to decrease to less than about one every two minutes. Once 50 μA was reached, the electrodes were left to condition for about six hours. Periodically, the gap size was checked, and data of I and V were taken for F-N plots. For a current of 50 μA, the gap voltage ranged from 1.80 to 1.95 kV, the average being 1.88 kV. From the F-N plots, β was determined, ranging from 313 to 386, the average being 350. The pressure was $\simeq 5\times10^{-8}$

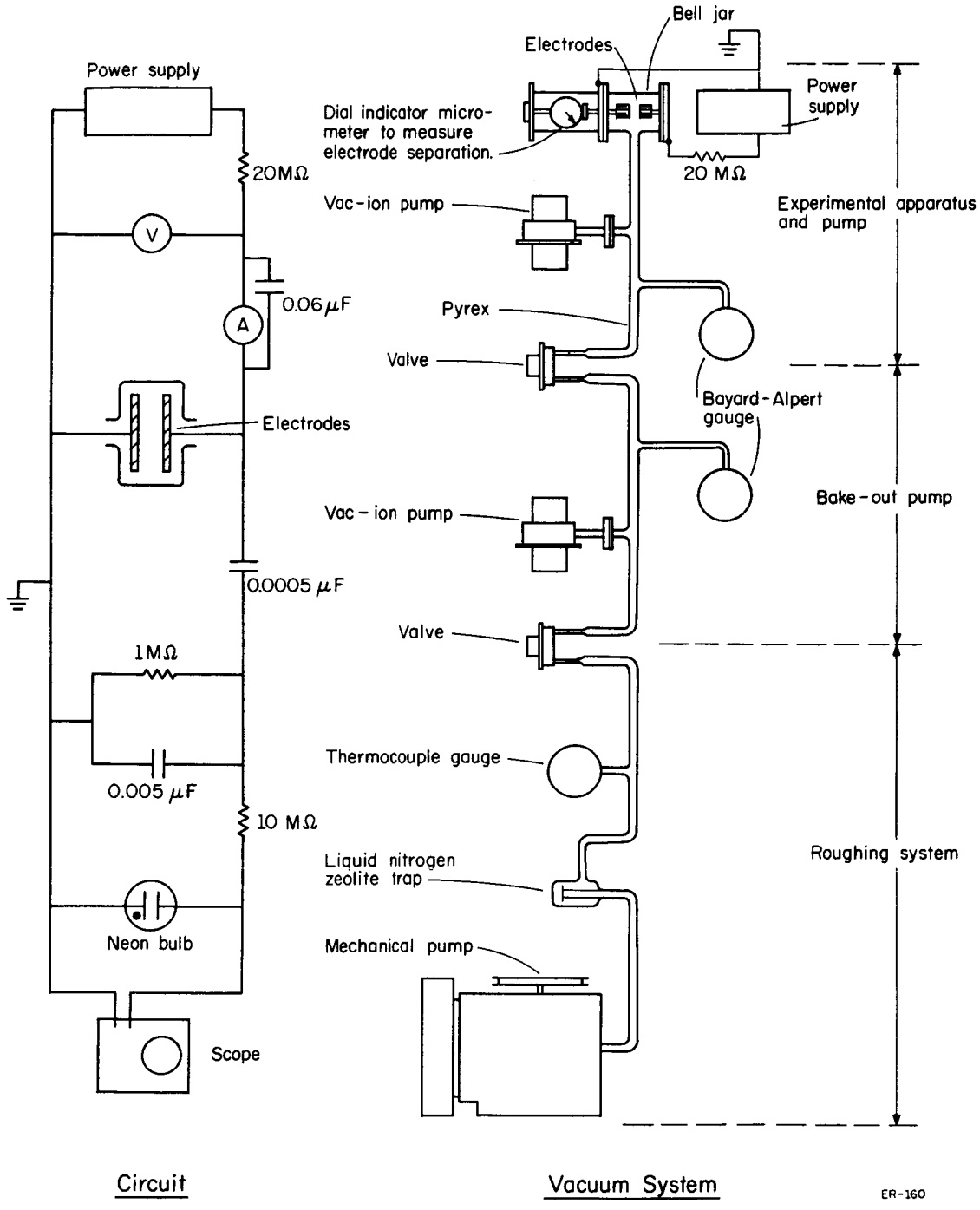

Figure 2.

Schematic diagrams of apparatus and circuits.

Torr. These results and those of subsequent runs described below are summarized in Table II.

Next, the polarity was reversed, making the anode disk Mo, and the cathode, Be. The current was increased to 35 μA, maintained steady for 1.5 hours, then raised to 50 μA and maintained steady for 6 hours (during which time the sparking rate became very small) before the measurements were started.

Set II: Be was first used as anode and the Mo disk with the teflon pad cemented to it as the cathode. Conditioning of this pair to 50 μA required 11 hours, and data were taken after maintaining a steady 50 μA current for 2 hours. When the polarity was reversed, conditioning to 50 μA required 7 hours and data were obtained after an additional 2-hour period at 50 μA.

Set III: The anode was Be and the cathode, Mo. Conditioning to 50 μA required 4.5 hours, and data were taken 5 hours thereafter. Upon reversing the polarity, 3 hours were required for the conditioning and data were taken 5 hours after reaching the 50 μA current.

Set IV: The anode was Be and the cathode, the Mo disk with the teflon pad. Prior to installation the teflon was examined under the microscope. The teflon had microscopic pin-holes in it and, in addition, a ragged edge protruding about 3 mils above the surface (as measured with an ohmmeter), along a portion of the disk's edge. Most of this pad protrusion was removed by adjusting the gap to 4 mils and operating for one minute at a current of 15 μA, but a small boss ¼ mil high remained. The behavior

of this electrode pair was erratic. A period of 17 hours was required to condition the electrodes to 50 μA. After operating at 50 μA and 1.1 kV for about 30 minutes with no breakdowns, the high voltage was turned off to permit gap remeasurement (touching the electrodes together to obtain the zero). Upon restoring the current to 50 μA, the gap voltage was found to have increased, but a burst of breakdowns soon occurred and the gap voltage dropped back to its usual lower value of 1.1 kV. This type of behavior did not occur constantly, but it was fairly frequent. It may have been due to some protrusion on the edge of the teflon which was erected by the electric field.

The electrodes were finally conditioned to the point where the current was 50 μA and only a small number of breakdowns occurred over a 6 hour period, after which data were obtained as shown in Table II.

Upon reversing the polarity, conditioning to 50 μA was achieved in 20 minutes. Although the initial voltage was 2.2 kV, after a large burst of breakdowns it dropped to 1.25 kV at 50 μA, remaining low thereafter. After 6.5 hours at 50 μA data were taken, as summarized in Table II.

Equations used to determine β

Field emission current:

$$I = \frac{(1.54\times10^{-6})\ \beta^2 V^2 A}{\phi\ t^2(y) d^2} \exp\left\{ \frac{(-6.83\times10^{7})\ \phi^{3/2}\ v(y) d}{\beta V} \right\} .$$

Taking $\log_{10}(I/V^2)$, we have:

$$\log_{10}(I/V^2) = \log_{10}\left[\frac{(1.54\times10^{-6})\ \beta^2 A}{\phi\ t^2(y)\ d^2} \right] - \frac{(2.96\times10^{7})\ \phi^{3/2}\ s(y) d}{\beta V} .$$

Plotting log (I/V^2) vs 1/V gives for the slope of the straight line:

$$\text{Slope} = \frac{d[\log_{10}(I/V^2)]}{d[1/V]} = -\frac{(2.96\times10^7)\,\phi^{3/2}\,s(y)d}{\beta}$$

where

V = electrode potential difference, volts,

I = field emission current, amperes,

A = emitter area, cm^2

d = electrode separation, cm,

ϕ = cathode work function, eV,

s(y) = slowly varying function of the electric field $\approx$ 0.9,

t(y) = slowly varying function of the electric field $\approx$ 1.1,

β = field at emitter tips/average field between electrodes.

$$\therefore \quad \beta = -\frac{(2.96\times10^7)\,\phi^{3/2}\,s(y)d}{\text{slope}} \quad .$$

Constants used in calculation: Work function of the cathode material.

Mo and Mo with teflon pad	ϕ = 4.20 eV
Be	ϕ = 3.92 eV.

Giving

Mo cathode	$\beta = 1.16\times10^6/\text{slope}$
Be cathode	$\beta = 1.05\times10^6/\text{slope}$

$$\text{Ratio}\ \frac{\beta_{Mo}}{\beta_{Be}} = 1.11 \quad .$$

Description of electrodes after the tests

Set I. Be-Mo

Be: The disk contained a number of large pits and many small ones. The large pits are attributed to spark damage which occurred because the current limiting resistance (between power supply and electrode) was small. The small pits were obtained when a 20 megohm current limiting resistance was added later. They were fairly evenly distributed over the surface.

Mo: About 20 large pits were found in an area at the edge of the electrode. There were no small pits, as were found on the Be. The large pits were probably caused by the spark damage that occurred with the small current-limiting resistance.

Set II. Be-Mo with teflon pad.

Be: Same electrode as used in set I.

Mo: Almost no pits were found on this electrode except at the edge of the teflon. Just at the edge of the teflon, a ring, consisting of many small pits, could be seen with a 10X magnifying glass. One may conclude that the effect of the breakdown discharges is to wear away the teflon at the edge. Five to 10 pits were found on the teflon itself and about two pits on the Mo surface.

Set III.

Be: See description of set IV.

Mo: A few pits, randomly distributed over the surface, were found.

Table II. Summary of Data and Calculations

Electrode Set	No. of runs	β_{ave}	Ratio	β_{range}	V at 50μA	V_{range} at 50μA	Pressure	$F_{crit.}=\beta\frac{V}{d}$
I. Plain disks								
Mo cathode	4	350	1.14	313-386	1.88 kV	1.80-1.95	5×10^{-8} Torr	1.3×10^{8} V/cm
Be cathode	4	306		273-336	1.86	1.70-2.00	1×10^{-8}	1.12
II. Teflon on Mo								
Mo cathode	4	298	2.48	267-340	2.24	2.2 -2.25	1.5×10^{-8}	1.31
Be cathode	5	120		105-141	2.14	2.05-2.20	$< 10^{-8}$	.51
III. Plain disks								
Mo cathode	5	262	1.21	236-312	2.11	1.95-2.35	5×10^{-8}	1.09
Be cathode	6	217		171-285	2.51	2.25-2.60	8×10^{-8}	1.07
IV. Teflon on Mo								
Mo cathode	3	303	1.53	271-322	1.28	1.12-1.52	$< 10^{-8}$	.76
Be cathode	3	199		170-226	1.22	1.20-1.25	$< 10^{-8}$	.48

Set IV. Be-Mo with teflon pad.

Mo: This electrode was covered with pits, with greatest concentration around the edge of the teflon. A region comprising a third of the teflon disk had been destroyed, leaving a black coating which was densely covered with many pits, while the undestroyed region had only 5 to 10 pits on it. The density of pits on the Mo metal fell off sharply with distance from the teflon.

Be: This disk also had a black-covered region of extremely high pit density corresponding to the destroyed part of the teflon pad on the Mo disk. Elsewhere on the disk, the pit density fell off more rapidly with distance from the teflon disk than it did on the Mo disk. In the region opposite the undestroyed portion of the teflon pad there were very few pits.

One may postulate that the black coating on the two disks in the region where the teflon was destroyed is due to the carbonization of the previously described ragged edge of the teflon disk. In both sets II and IV, the pitting occurred mainly at the edge of the teflon.

Remarks:

The data in Table II show that the teflon may have an adverse affect on the voltage holding capabilities of the electrode pair and upon the interelectrode current. This effect was found to be large in the case where a protrusion seems to have initiated carbonization and small in the case where the teflon edges were smooth and well-fastened to the Mo disk. The improvement in voltage between set I (without teflon and set II (with teflon) is not regarded as significant. On the other hand, the gap voltage was halved by the presence of carbonized teflon in set IV.

It appears that the ¼ mil teflon boss which remained on the Mo electrode in set IV may have contributed to the onset of carbonization, suggesting that a smooth teflon coating may be a requirement for good voltage-holding capability. In the practical use of teflon scuff pads, consideration should be given the possibility that the spinning gyro ball may scuff the teflon sufficiently to cause deterioration in the electrical breakdown characteristics.

The data of Table II indicate that the teflon pad may affect the value of field enhancement factor, β. For sets I and II, the addition of the pad was associated with a decrease in average β by 60% with Be as cathode and by 25% with Mo as cathode. On the other hand, for sets III and IV, the addition of the teflon was associated with an increase in β by 15% when Mo was the cathode material and a decrease of β by 10% when Be was the cathode material. Thus, our results on the effect of the teflon on β are inconclusive.

In set IV there is some evidence that conducting slivers of material were raised up and tended to bridge the gap under the action of the electric field. In several instances, after application of the high voltage considerable breakdown activity would ensue, causing the voltage to fall below the initial value. This might be interpreted on the basis of the raising of metallic whiskers previously lying on the surface of the cathode. In one case the gap voltage dropped to zero even though the spacing remained at 2 mils. A slight jar removed the short, as though the sliver had been knocked off. In closing the gap it was sometimes noted that protrusions would be crushed in the process of bringing the electrodes together.

APPENDIX F

Field Emission from a Multiplicity of Emitters on a Broad Area Cathode

by

H. Tomaschke and D. Alpert

It has been well established[15-18] that for clean metallic electrodes in high vacuum, the predischarge current from a broad area cathode follows an exponential dependence on the applied voltage, and is explained on the basis of the Fowler-Nordheim theory for field emission. In a recent paper,[15] we have adduced evidence from our own experimental results and others[19-21] have shown that field emission current originates from a number of separate localized emission sites on the cathode; these sites were shown to be whisker-like projections on the cathode surface at which the electric field is greatly enhanced.

For a single projection, the enhancement factor, β, the factor by which the local electric field at the tip exceeds the average field, can be determined from a Fowler-Nordheim (F-N) analysis of field emission current and applied voltage. In the case of parallel-plate electrodes, the field at the tip of a projection can be written as

$$F = \beta\ V/d$$

where V is the applied voltage in volts and d is the gap spacing in cm. In terms of these parameters, the Fowler-Nordheim expression for the current, I in amperes, takes the form

$$I = JA_E = \frac{A_E C_1}{\phi} \left(\frac{\beta V}{d}\right)^2 \exp\left[-6.83\times10^7\ \phi^{3/2}\ v(y)\ \frac{d}{\beta V}\right] \qquad (1)$$

where A_E is the emitting area in cm^2, J is the current density in A/cm^2, C_1 is approximately a constant, ϕ is the work function in eV, and v(y) is a slowly varying function.[22] A plot of log $I(d/V)^2$ *vs.* d/V should result in a straight line whose slope is given by:

$$-C_3\phi^{3/2}s(y)\ d/\beta$$

where $C_3 = 6.83\times10^7 \log e = 2.96\times10^7$, and s(y) is a slowly varying function,[22] which for the range of experimental interest can be approximated by the numerical factor 0.9. Thus the slope of the curve which results from an F-N plot uniquely determines the enhancement factor, β.

If the total current were supplied by several protrusions, each with its own enhancement factor, one would not expect, *a priori*, that the sum of such curves would result in a straight line on a similar logarithmic plot. Yet, as shown in Figure 3, the experimental data from broad area electrodes consistently result in a straight-line Fowler-Nordheim plot, as if the entire current originated at a single point; indeed, it has been argued[16] that this is the explanation of the single exponential which is observed. On the other hand, very strong direct experimental evidence indicates that for the data such as that shown in Figure 3, the current originates from a multiplicity of points, representing a distribution of enhancement factors, β_i, and emitting areas, A_i.

In an attempt to reconcile these observations, a computer analysis was undertaken to examine on theoretical grounds the nature of the curve to be expected from the summation of the field emission currents from a

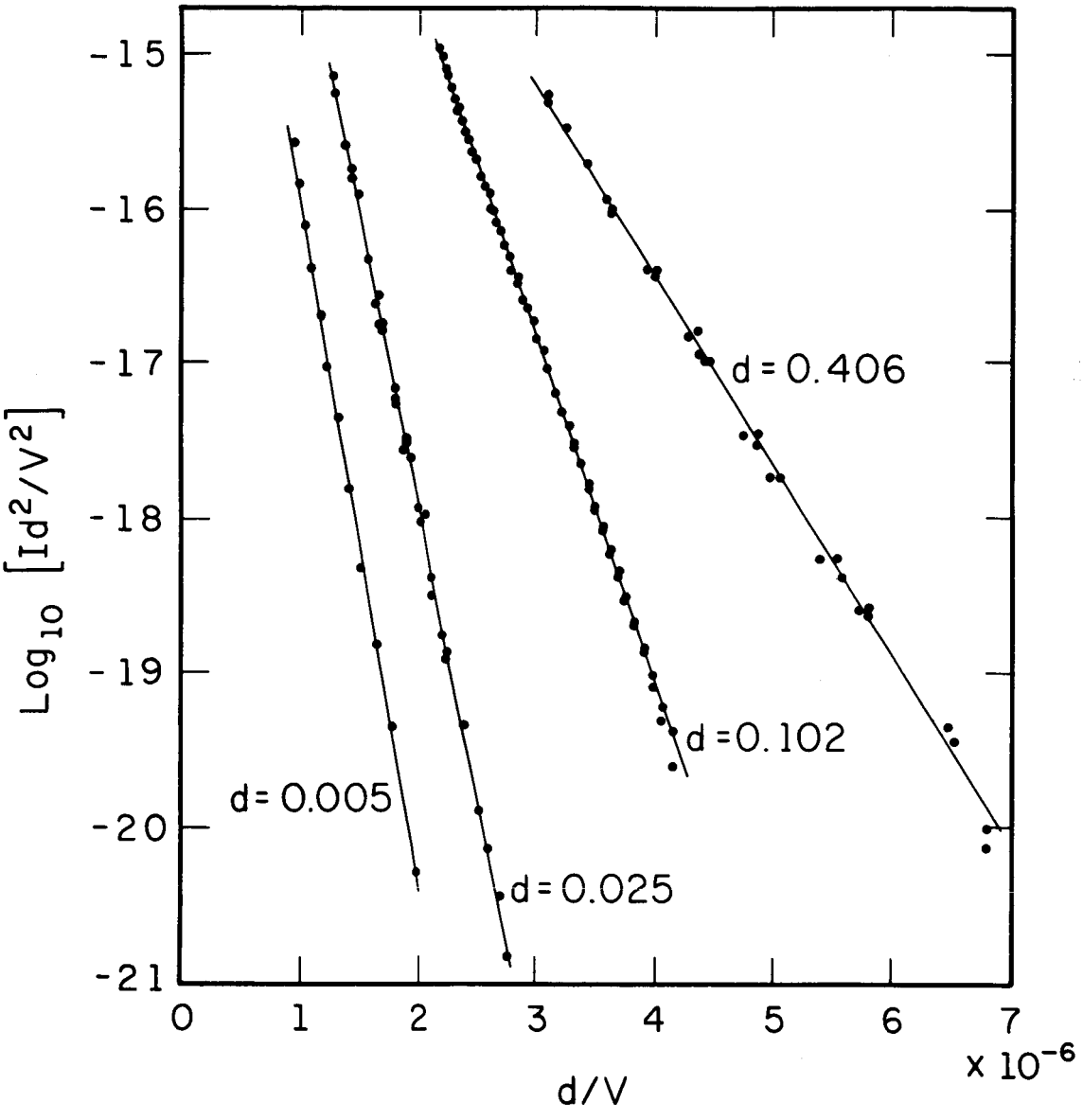

Figure 3.

Typical Fowler-Nordheim plots of the field emission current between clean parallel tungsten electrodes for various designated gap spacings (in cm), V in volts, I in amperes.

distribution of separate emitters. A digital computer program was written to compute the total emission from a group of emitters, randomly selected as to enhancement factors, β (within the range of 70 to 150), and emitting area, A_E (within a range that varied by a factor of 100). The number of emitters in a given group varied from 2 to 100. For each group, the current from each emitter point was calculated for a given value of the average field, F_0. The contributions from the ensemble were then added and the total current plotted as a function of F_0 in the typical F-N manner.

In each of the groups considered, the logarithmic plot obtained from the summation of the calculated contribution of the emitters resulted in a stright line. A representative group of emitters is characterized by the properties listed in Table III. The F-N plot which represents the summation of current from the several points is shown in Figure 4. It is immediately seen that any departure from a straight line is so small as to be undetectable. If one then assumes that the resulting curve originates from a single, "effective" point, one can readily compute an effective β and an effective A_E which characterize the properties of the ensemble of points in the group.

When the group chosen included four or more points, it was typically found that the effective enhancement factor, β_{eff}, had a numerical value which was a weighted average, strongly dominated by the higher β's in the group. The effective area, as would be expected, was generally larger than the area of any individual emitter, but less than the combined sum. Even when only two emitters were selected with random β's and area, the F-N curve was typically a straight line. In this case, the value of β_{eff} was equal in value to the enhancement factor of the sharper of the two points.

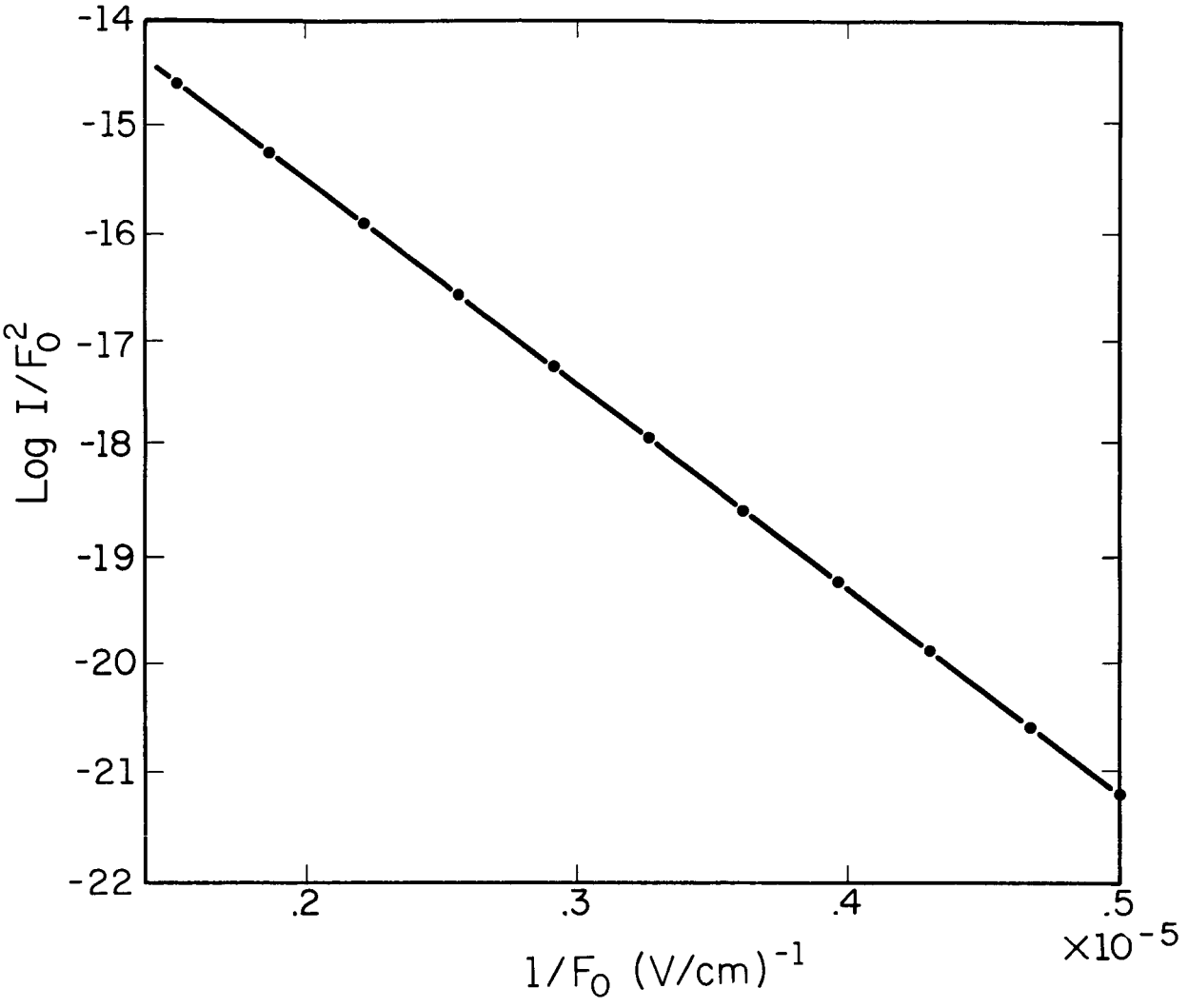

Figure 4.

Fowler-Nordheim plot of the calculated combined currents from the group of emitters listed in Table I.

Table III. Individual enhancement and area factors for ten emitters and the calculated effective values

	β	Area(cm^2)
Individual Values	143	$.189 \times 10^{-12}$
	114	.774
	113	.632
	131	.416
	108	.321
	102	.816
	139	.938
	144	.936
	117	.901
	100	.713
Effective Values	137	3.670×10^{-12}

The nature of the F-N curve to be expected from two emitter points is especially interesting since it provides insight into the physical reasons for the results described above. In the general case, one would expect that the individual F-N curve for each of the two emitters would be a straight line and, unless the enhancement factors were identical, these would intersect at some point. Thus, strictly speaking, the current-voltage dependence would not be represented by a single, straight line. However, it is important to note that if the two emitters are of more or less equal emitting area, and the β's, i.e., the slopes, differ by only a few percent, the individual curves will be almost parallel to each other. Hence, the amount by which the sum of the two curves departs from a straight line will be negligible, especially since the range of values for the applied field is limited. (Experimental values of the applied voltage typically cover a range which varies at most by a factor of two.) On the other hand, if the enhancement factors of the two points differ significantly, the fraction of the total current supplied by the blunt point is very small, and the curve representing the total emission is virtually identical with that for the sharper projection. To give a specific example, consider two projections of equal emitting area but of different enhancement factors, $\beta_1 = 100$, and $\beta_2 = 150$. In this case, the percentage of the current contributed by the blunt point ($\beta = 100$) is very small. When the average field is one-half the value at which breakdown would occur, point (1) contributes only .01% of the total current (see Figure 5). As the field is increased, the percentage of the total current originating at the blunt point increases, but even when the local field at the sharper point reaches the critical breakdown value, this percentage is only 1% of the total. To contribute enough

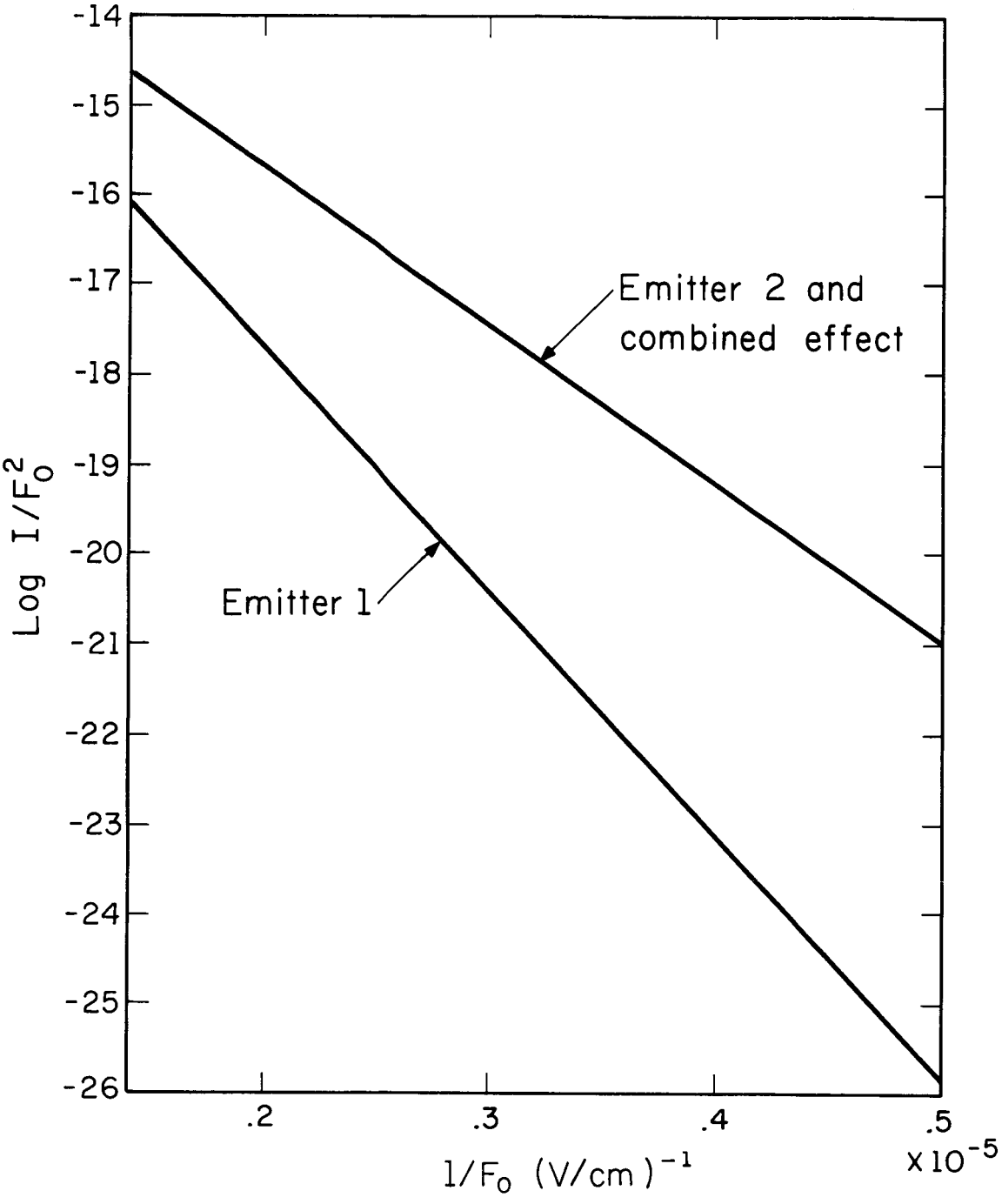

Figure 5.

Fowler-Nordheim plots of currents from two different emitters and their combined current. $\beta_1 = 100$, $\beta_2 = 150$, $A_1 = A_2 = 10^{-12}$ cm^2.

current to affect the F-N curve, i.e., to have the two individual F-N curves intersect in the region of observation, the emitting area of the blunt point would have to be approximately two thousand times larger than that for the sharper (β = 150) emitter. Since the general shape of the two points would be similar in terms of their height-to-base ratios this would require that the blunt point be fifty times larger in linear dimensions than the sharper projection. While such a disparity in size is not out of the question, it seems highly unlikely and hence it is not surprising that it is not experimentally observed.

From such calculations, carried out for a wide variety and multiplicity of emitting points, it is first of all demonstrated that a straight line Fowler-Nordheim plot is to be expected from virtually any realizable multiplicity of emitting sources. The effective area, as deduced from the composite F-N curve, provides relatively little information regarding the actual size of the individual emitters. However, the effective enhancement factor as obtained from the composite F-N plot gives a very good estimate of the enhancement factors of the individual projections most likely to play a role in the next breakdown.

The Role of Submicroscopic Projections in Electrical Breakdown

by

H. Tomaschke and D. Alpert

ABSTRACT

Observations with an electron microscope and with a modified field emission microscope verify the formation of submicroscopic, whisker-like projections on the cathode surface, thus lending additional supporting evidence for the association of electrical breakdown with field emission from such sites. Several mechanisms for the formation of whiskers are identified. The predischarge current, with which the initiation of breakdown is associated, is observed to exhibit large fluctuations in the presence of contamination on either or both electrodes, and a tentative explanation is set forth in terms of a special proliferation of smaller protuberances.

I. Introduction

Recent publications have provided strong support for the association of electrical breakdown with field emission from submicroscopic projections on broad area electrodes. Based on the enhancement of the electric field at such protuberances on the cathode, this physical explanation has been substantiated by (1) measurement of current-voltage relationships,[23,24] (2) direct observations in an electron microscope,[25] and (3) magnified images of electron emission patterns.[26] The present work,

initiated in 1961,[27] has combined all three of the above general approaches on cathodes of the same physical dimensions and characteristics. The results reported here had a direct bearing on the development of the model reported earlier[23] and are corroborative in an important sense to the other references cited above. That is, the observations provide further evidence for the existence of properties of submicroscopic projections on a broad area cathode. In addition, we report certain results which are quite unique and which provide insight into the mechanisms for the formation of such projections.

The cathode in each of the experimental approaches in our work was the blunt end of a three mil (.007 cm) tungsten wire. Such a cathode can be considered a "broad area" electrode by comparison with the experiments of Dyke and his co-workers[28,29,30] who first established the field emission model for breakdown using a point-to-plane geometry with single crystal tungsten cathodes 100 to 1000 times smaller. Furthermore, such cathodes are considered "broad area" in another sense: in the experiments on current-voltage relationships, the gap spacing was comparable to or smaller than the cathode diameter, and hence the macroscopic field configuration is specifically comparable to that with much larger dimensions.

II. Electron Microscope Studies

These experiments were first initiated to confirm directly the existence of submicroscopic protrusions, and if possible, to establish the mechanisms for their formation or removal. The choice of electrodes of small dimensions was dictated primarily by the requirement that the entire cathode be inserted into the electron microscope.

Initially, it was hoped that the entire sequence of experiments could be carried out within the microscope; that is, current-voltage runs up to the point of breakdown, with direct observation of the surfaces before and after breakdown. It soon became evident, however, that the electron microscope vacuum system contained so much oil and other contamination that the electrical characteristics were not reproducible and had little relationship to those reported with ultrahigh vacuum.[23] The configuration was therefore modified so as to support one of the electrodes (usually operated as the cathode) either on a modified specimen holder for insertion into the microscope or on a demountable flange for insertion into an ultrahigh vacuum system. Thus, in the sequence of experimental events, the cathode was alternately inserted into the ultrahigh vacuum system for preparation of the electrodes or for current-voltage runs; then it was transferred into the electron microscope for observation at any point in the sequence, either before or after electrical breakdown had taken place.

The demountable electrode was a fine (.007 cm dia) tungsten wire spot-welded to a heavier tungsten hairpin filament which permitted the tip to be heated to a maximum temperature of 1600°C. This structure was mounted on a modified specimen holder as shown in Figure 6 for insertion into the electron microscope, an RCA Model EMU-2E. The resolution of the microscope, as used in this investigation, was about 50 Å and the depth of focus approximately 2000 Å. A shadow profile of the electrode was normally displayed on the screen at a magnification of approximately 10,000. The image was photographed in overlapping views, and enlarged

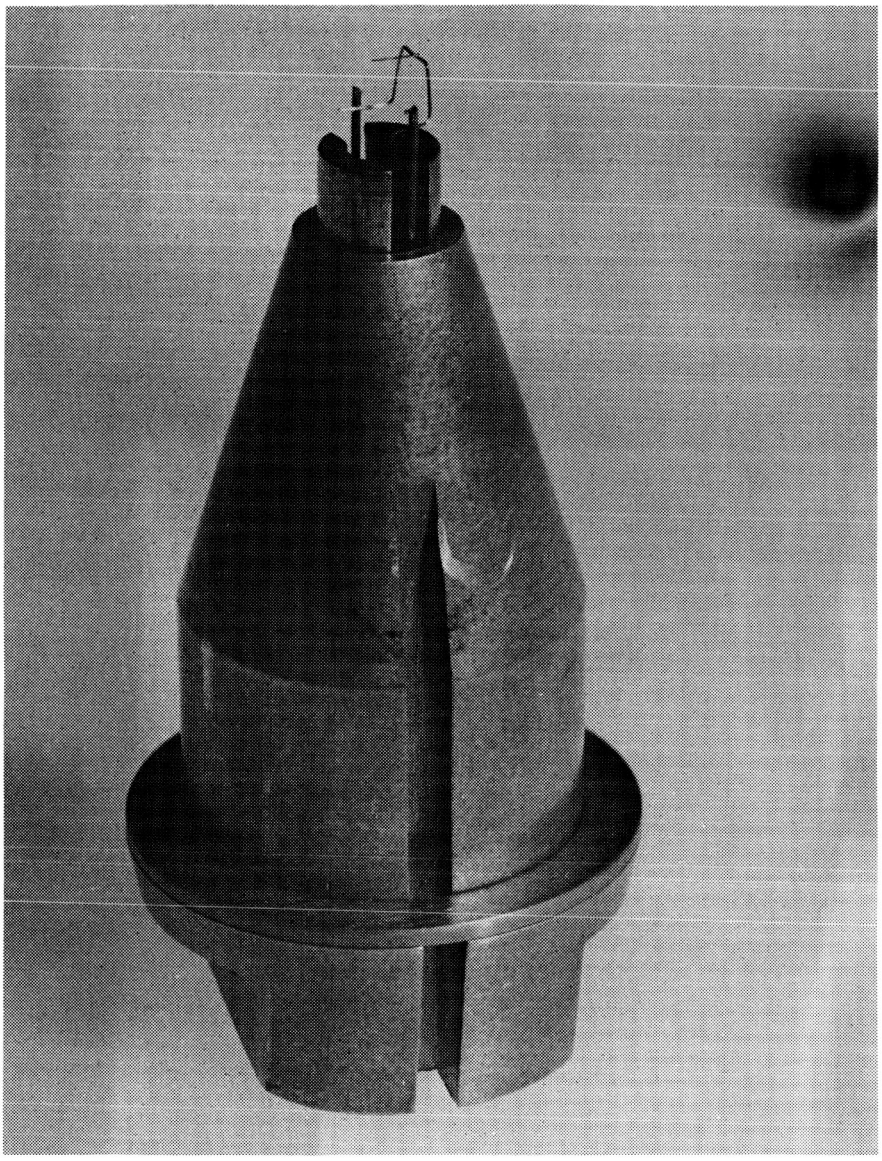

Figure 6.

Electrode mounted in the modified specimen holder for viewing in the electron microscope.

prints (2x) were made from the resulting photographic plates. By tracing over these it was possible to identify changes in the profile outline and to verify scale magnification.

In order to set the zero gap reading, the cathode was brought into electrical contact with the tungsten anode. One of the most interesting of the observations involved the microscope inspection before and after touching the electrodes together, as shown in Fig. 7a and 7b. Although the forces involved were very small (estimated to be a few grams) the localized stresses were obviously sufficient to generate whisker-like protrusions. While certain of these might have been formed upon pulling the electrodes apart (possibly following a cold weld), it seems evident that the projections identified with an arrow in 7b are the result of compressive stresses. The formation of such protrusions undoubtedly accounts for the observations of Miller and Farrall[31] that "bringing the electrode faces into physical contact appeared to remove much or all of any conditioning." The size of the protrusions shown in Figure 7 are of the order of 1 micron in height and 0.1 micron in diameter. It was found that heating the cathode to about 1600°C for 2 minutes was sufficient to blunt the sharp projections caused by physical contact between the electrodes. After heating, the appearance of the electrode surface was similar to that shown in Figure 8a.

After a series of current-voltage runs, the cathode surface typically revealed the formation of several sharp projections. (See Figure 8a and 8b.) After certain runs, the careful inspection of high magnified views of localized areas also verified the disappearance of one or more of the points, presumably in the course of the breakdown process. It can

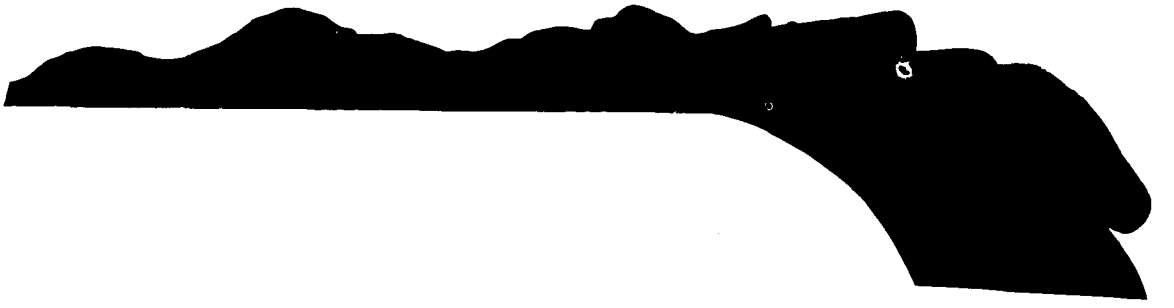

Figure 7a.
A section of the electrode showing the initial profile.

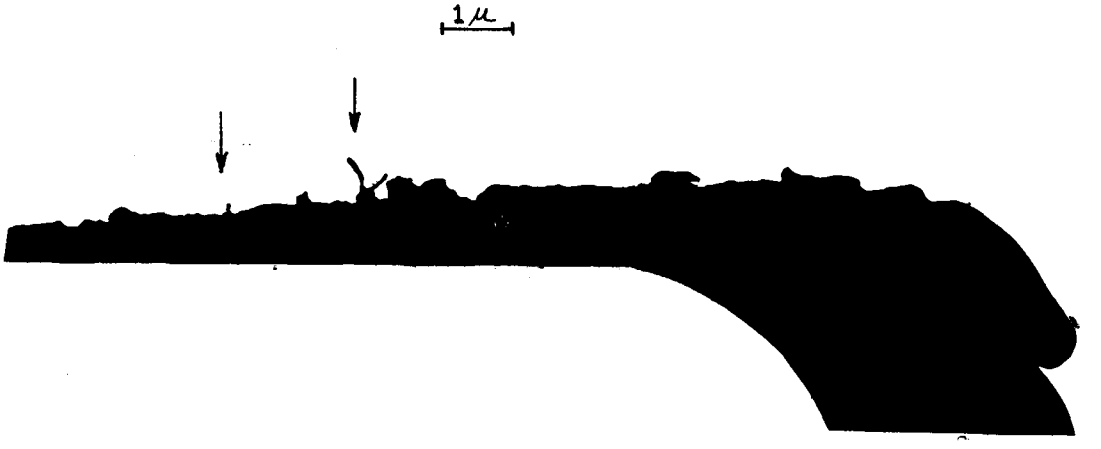

Figure 7b.
The same section after physical contact
with the opposing electrode.

Figure 8a.
Appearance of the electrode surface after heating.

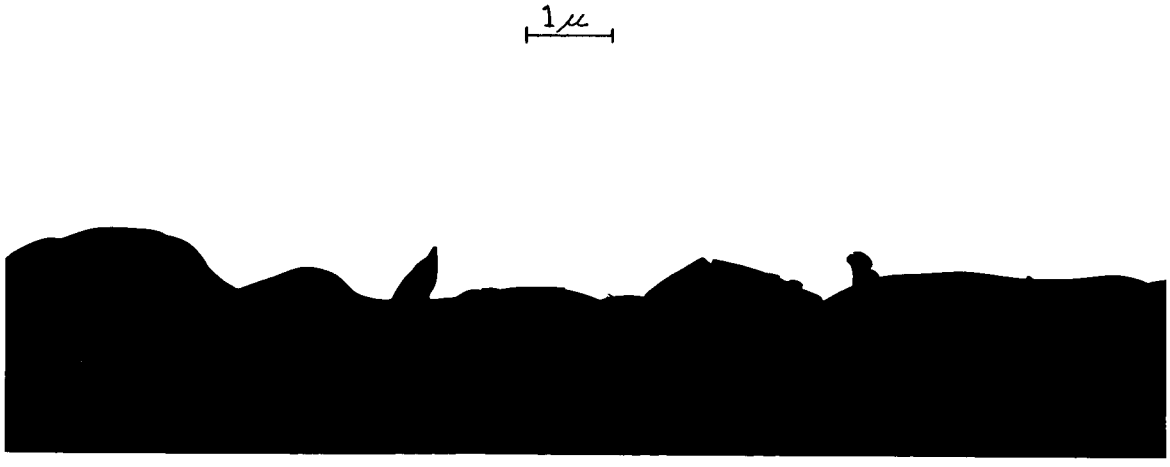

Figure 8b.
Electrode projections created by electrical breakdown.

be seen from Figure 7 and Figure 8 that the shape of the projections varied widely; it is difficult to identify any particular structure or orientation. However, the size and shape of the sharper protrusions were roughly in accordance with predictions from other studies,[23,32] i.e., the height varying between 10^{-5} cm and 10^{-4} cm, and the diameter being of the order of one-fifth to one-tenth of the height.

III. Current-voltage Characteristics for Small Gaps

To correlate the electron microscope observations with the electrical properties of the electrodes, a number of measurements of the predischarge current-voltage characteristics were carried out. Frequently these were taken with increasing applied voltage up to the point of breakdown, as indicated by a visible flash. Such measurements were made in a more or less standard demountable ultrahigh vacuum glass-metal system, with one of the electrodes mounted on an adjustable bellows to vary the gap spacing and the other electrode locked into position but transferrable to the electron-microscope.

As shown in Figure 9, a close-up view of the electrodes, the movable electrode was initially a relatively massive tungsten rod 0.100 inches in diameter, brazed into a stainless steel support, and machined and electropolished. In this arrangement, the adjustable electrode (typically the anode) could not be outgassed at high temperatures. When it was found, during the course of these experiments, that contamination of the anode could play a significant role, the tungsten rod was replaced by a hairpin tungsten wire (.025 cm dia) which could be raised to a high temperature.

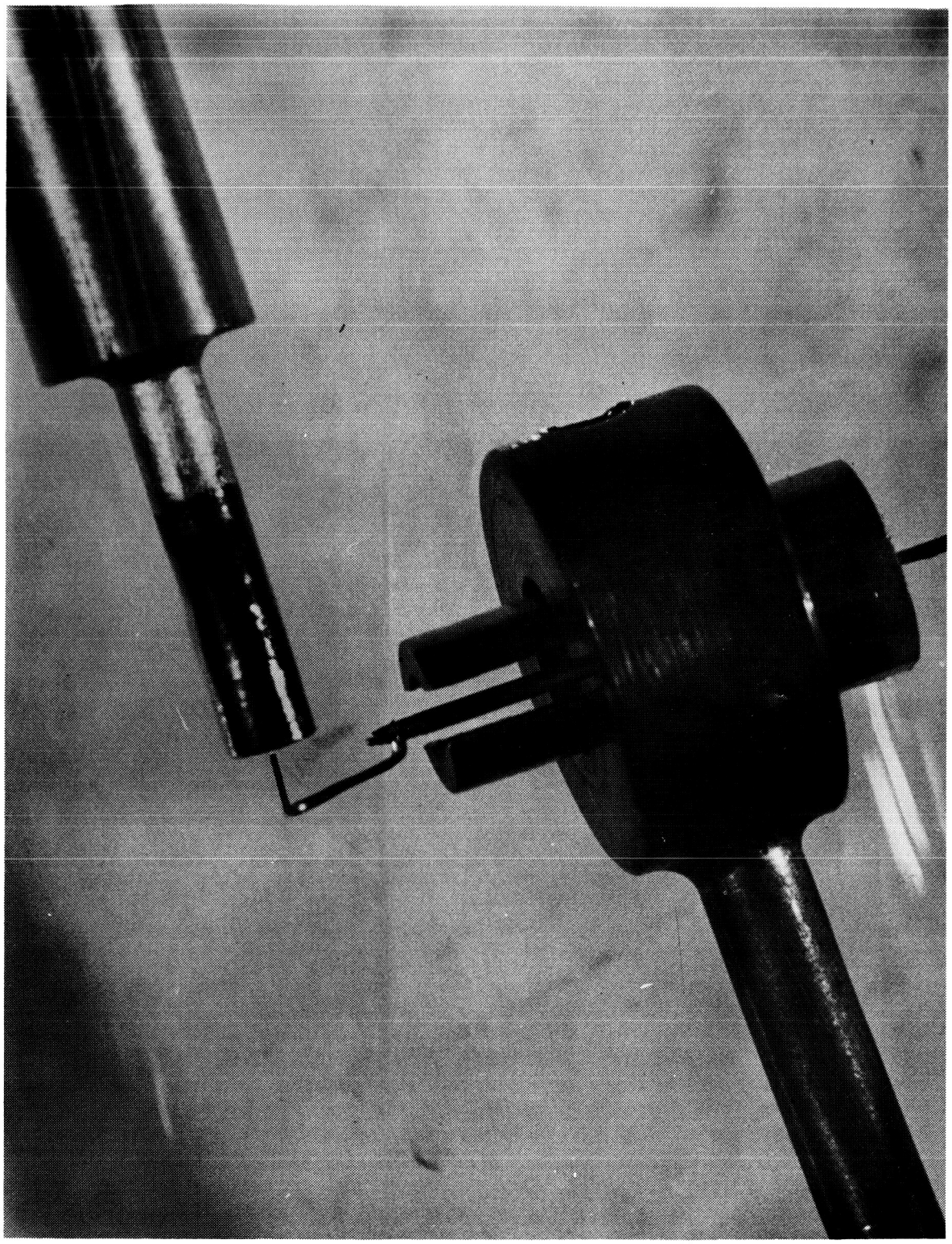

Figure 9.

Close-up view of the electrodes.

As indicated previously, to set the zero gap spacing (gap spacing was of the order of .005 cm) the electrodes were initially brought into electrical contact. Since this procedure itself was soon shown to produce a significant growth of protrusions, the method for measuring gap spacing was then modified. In later experiments, an externally mounted optical microscope was utilized to estimate the separation by comparison with the known dimensions of the smaller electrode. Field emission currents were determined by measuring the voltage drop across the cathode-to-ground resistance. The minimum measurable current was about 10^{-10} A.

The current-voltage characteristics for these small gaps fell into two quite distinct categories of behavior, the discovery of which first confused the situation but later contributed significantly to the understanding of predischarge currents and the role of micro-projections. These two modes of behavior are designated as the "F-N" mode and the "unstable" mode. An attempt to make a Fowler-Nordheim (F-N) plot of the current-voltage characteristics resulted in a curve such as that shown in Figure 10.

For lower values of voltage, up to about 4000V, and currents up to about 1×10^{-7}A, the curve followed an F-N dependence as shown. Although the current in this mode was relatively stable it did exhibit sizeable fluctuations. Observations of these fluctuations on an oscilloscope revealed a random modulation as shown in Figure 11. Two interesting features may be noted. First of all, the fluctuations give the appearance of a flat-topped or square-wave modulation of random duration, with individual on or off times ranging from many milliseconds down to the lowest value permitted by the instrumental time constant of the coupling circuitry. (In this case down to 0.1 milliseconds but in other observations down to microseconds.)

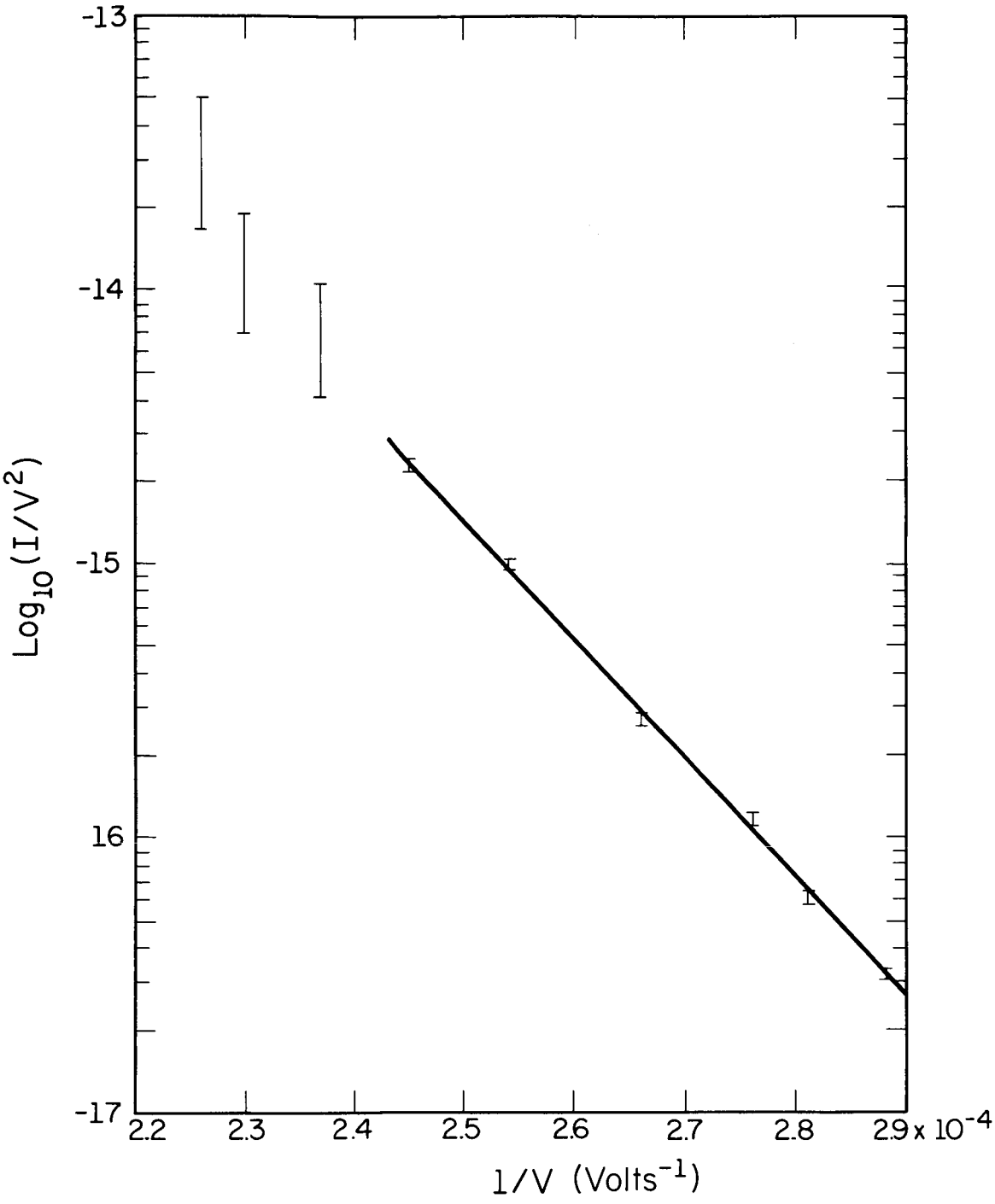

Figure 10.

A typical plot of I/V^2 vs 1/V showing the "F-N" region and the "unstable" region.

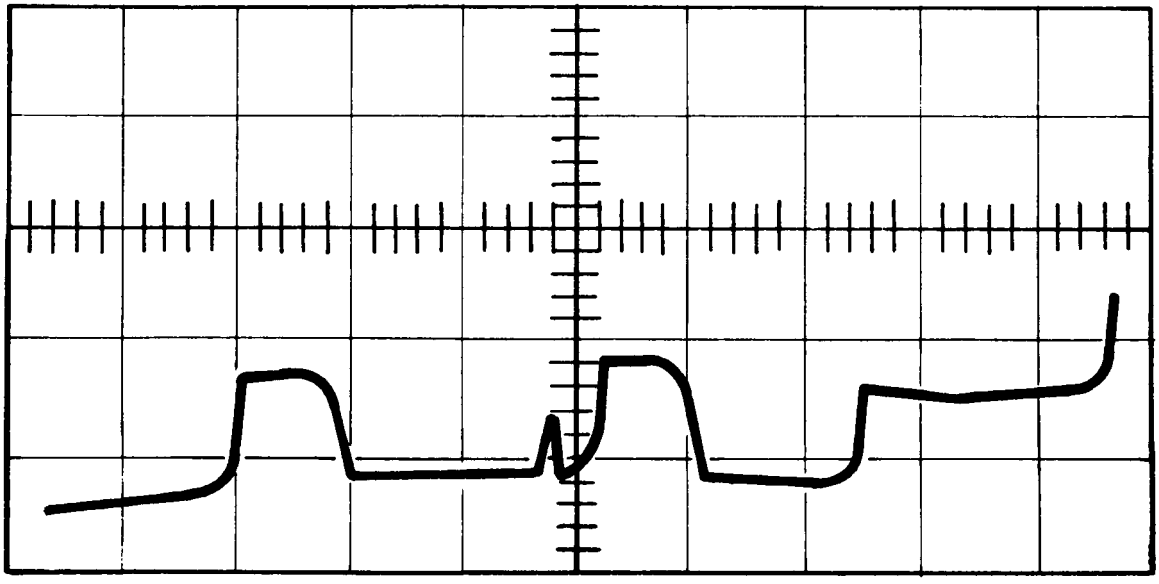

Figure 11.

Tracing of an oscilloscope picture of current pulses observed in the "unstable mode." Sweep speed 2 ms/cm, amplitude 2×10^{-7} amp/cm.

A second feature, as suggested by the spread of points on the F-N curve, is that the amplitude of the modulation, which was typically several percent of the total current, was roughly proportional to the average current. An explanation for these fluctuations, associated with the adsorption and desorption of atoms on cathode emitter sites, is discussed in the next section.

As the applied voltage was further increased, the current became highly unstable with large fluctuations in the average value, although no flashes or other visible evidence of breakdown were observed. In this region it was no longer possible to extend the F-N plot. The fluctuations in the reading of the current were comparable to the reading itself. If the voltage were again lowered to the field emission region, an exponential characteristic was again observed, but it was typically different in slope from the previous curve.

One of the interesting corollary results of this investigation was obtained by inspecting the cathode in the electron microscope after several minutes of operation in the unstable mode. This revealed a very large proliferation of whisker-like projections, usually smaller (approximately 0.1 micron in length) but in places so numerous as to present an almost lace-like pattern on the electron microscope screen (Figure 12). (In passing, it might be noted that similar projections were produced when the polarity was reversed and the electrode was operated as the anode in the unstable mode.)

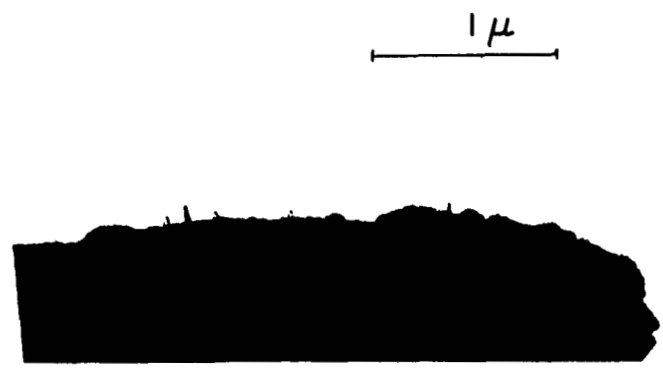

Figure 12.

Whisker-like projection found on the electrode after 15 minutes operation in the unstable mode.

In order to determine what effect, if any, the condition of the anode surface* might have on the current fluctuations in the unstable mode, the tungsten rod was replaced by a tungsten hairpin loop so as to be able to remove contamination by direct heating of the anode. It was again found that cleaning only the cathode did not eliminate the unstable condition. However, after both anode and cathode were heated to approximately 1600°C, the current followed a Fowler-Nordheim relationship right up to the point of breakdown. The calculated local field at breakdown was about 6×10^7 V/cm, in agreement with earlier results with large area tungsten electrodes.

This association of the unstable current mode with the condition of the electrode surfaces was further verified by exposing previously clean electrodes either to the atmosphere or to oxygen at a pressure of 10^{-6} Torr. Current fluctuations immediately reappeared; to eliminate them, it was necessary to reheat the electrodes to 1600°C. What seems particularly significant is that the condition of the anode has such an important effect on the unstable mode of operation, which is here seen to be associated with the proliferation of small whisker-like projections.

---

*This line of investigation was suggested in part by the results of Pivovar and Gordienko[33] relating the initiation of so-called "microdischarges" to electrode surface conditions. Indeed, some features of the unstable mode observed in our work are similar to the behavior described as "microdischarges" by Pivovar and Gordienko, and our explanation may be applicable to their observations.

A tentative picture which emerges from our experimental observations is as follows. The presence of an oxidized or otherwise contaminated anode provides a condition for the very sizeable production of ions[34] at the anode surface due to electron bombardment. These ions strike the cathode with energies corresponding to the total applied voltage between the electrodes and create sites for the growth of whiskers which are rather different in physical characteristics from those formed by other mechanisms. Some of these whiskers are presumably created with an enhancement factor such that the local field exceeds the critical field and they are rapidly destroyed. The size of these micro-projections are at least 10 times smaller and the volume of material is therefore 1000 times less than those usually associated with breakdown. The discontinuities in current can be attributed to a sequence of minor breakdowns at random intervals, the smaller size of the projections accounting for the fact that visible flashes are not observed.

IV. Modified Field Emission Microscope Studies

Much of the interesting and valuable work on field emission and electrical breakdown carried out by Dyke and his colleagues[28,29,30] were carried out with a conventional Mueller field emission microscope (FEM) incorporating a tungsten point cathode. The results of Brodie and Weissman[26] indicated that a similar tool could be used for broad area cathodes. The present studies of field emission patterns from a blunt cathode were carried out by substituting, for the point-emitter in a conventional FEM, a tungsten cathode of the same size (.007 cm dia) as those used in the electron-microscope studies. When the applied voltage was then

raised to a sufficiently high value, field emission was drawn to the anode, a metal-backed fluorescent screen, thus providing a magnified image of the regions of the cathode from which the electron current originated. This made it possible to study simultaneously the current-voltage characteristics and the properties of localized emitting sites.

The experimental arrangement involved standard ultrahigh vacuum techniques. Typical treatment included a 400°C bakeout of the entire system, followed by heating the cathode tip and its hairpin support to about 1600°C. After a careful outgassing of this type, the system could be maintained at pressures below 10^{-9} Torr for the duration of the run.

A photograph of a typical emission pattern is shown in Figure 13. This was taken with a total emission current of approximately 10^{-6} A, and an applied voltage of about 10^{4} V. The total pattern was characteristically made up of a number (from one to ten or more) of well-defined patches of illumination, each patch being attributed to a given projection on the cathode. With commercially drawn tungsten wire as the cathode material, the image from a given site never produced the symmetrical pattern associated with a rounded single crystal point-emitter. Such symmetrical patterns were observed only in one experiment, in which the cathode was fabricated by vapor deposition of the tungsten in an effort to attain an uncontaminated source.

As the applied voltage was raised, a new illuminated patch would appear on occasion, as if a protrusion had been created or suddenly elongated. The occurrence of breakdown was typically accompanied by the disappearance of one or more patches, and occasionally by the appearance

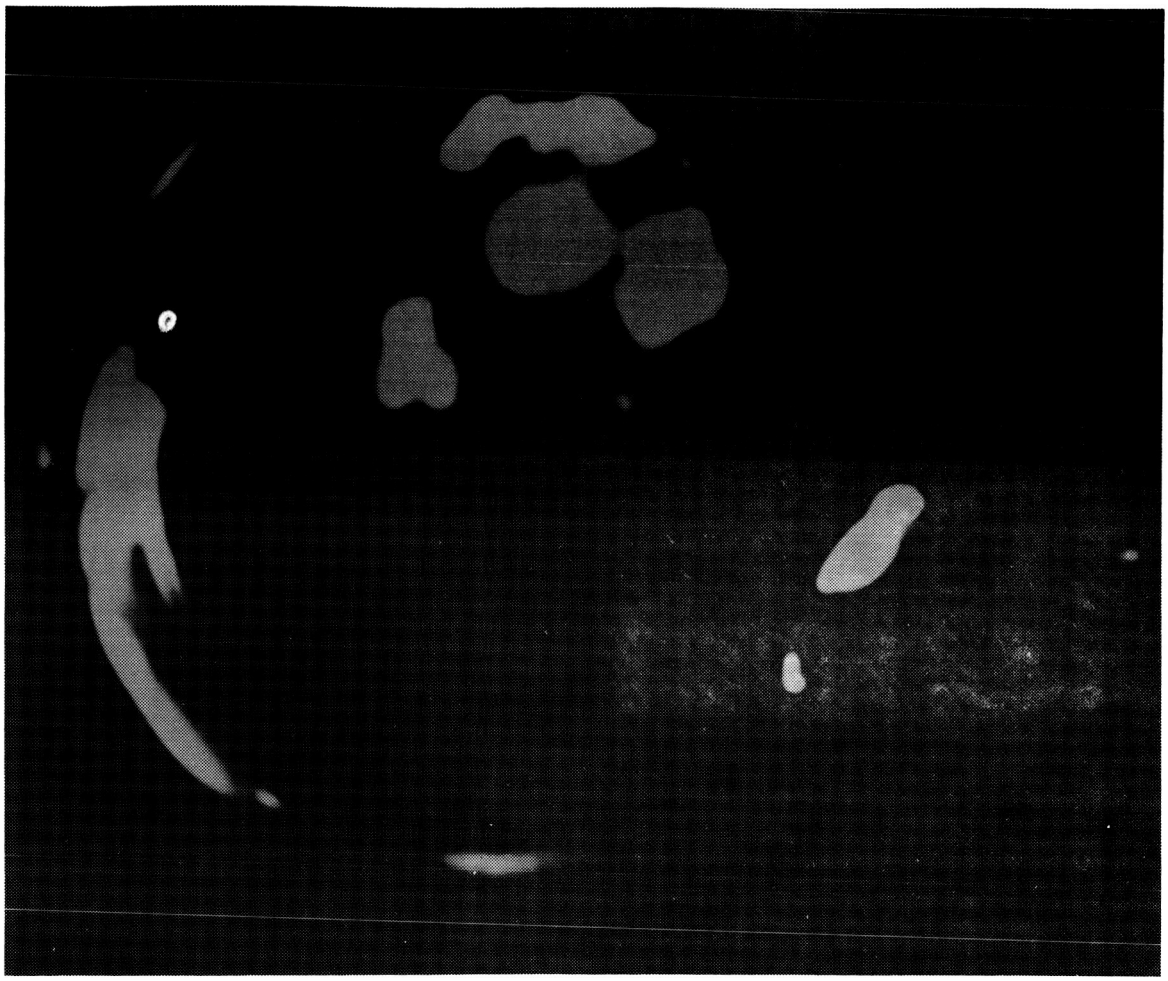

Figure 13.

Typical pattern observed with the modified field emission microscope.

of new emission sites. Following the disappearance of any or all of the sites, new sites could in any case be generated by raising the applied voltage.

The current-voltage characteristics observed with the modified FEM were similar in general character to those described for broad area electrodes.[23] One of the most interesting was the observation that the current followed a Fowler-Nordheim relationship quite independent of the number of emitting sites. As the total emission current increased with increasing applied voltage, the brightness of each of the major patches of illumination became correspondingly more intense. Although the F-N plot of the current-voltage characteristics in such a run yielded a straight line, it was demonstrated that several projections were contributing to the total emission from the cathode. This is at variance with the conclusion[24,35] that a straight line Fowler-Nordheim curve necessarily implies a single emitting source, and calls for a different explanation.[36]

The current-voltage characteristics were stable and reproducible, but random current fluctuations were observed which were very similar to those described for the small gap electrodes when operating in the "F-N" mode. The observation of the FEM pattern at higher fields did not show an enhanced production of randomly located whiskers as had been definitely indicated with the small gap electrodes. Rather, the fluctuations in current were found to be accompanied by a flickering of localized spots within the "patches" of illumination referred to above. These small bright spots periodically disappeared and then reappeared, typically in precisely the same location. By monitoring the light from such a spot with a light-sensitive detector and comparing the resulting signal with that due to the

total emission current, a direct correlation in time was ascertained. The fluctuations in both the light intensity of a given spot and the total measured emission current produced flat-topped pulses on the oscilloscope trace. These fluctuations are similar to those observed by Brodie.[37] His explanation that the "winking" spots are due to the alternative adsorption and desorption, at a given site, of individual atoms or molecules seems clearly justified.

The observed fluctuations in the current in the modified FEM were clearly associated either with gas impurities in the vacuum system or bulk impurities in the commercially drawn tungsten wire from which the cathode was constructed. Instabilities were greatly reduced, either if the cathode was outgassed for long periods of time at very high temperatures or when a sample of ultra pure tungsten was substituted as the cathode material.

V. Summary

The results presented here give additional supporting evidence for the model for the initiation of electrical breakdown based on field emission from sharp submicroscopic projections. The electron microscope observations served to identify three mechanisms for the formation of such whiskers: (1) the deformation of the electrode surface associated with direct mechanical contact, (2) the breakdown process itself, and (3) the transfer of charged particles from a contaminated electrode.

Fluctuations in predischarge currents have been associated with contamination of either or both electrodes. One source of these fluctuations seems clearly to be attributable to the adsorption and desorption of

atoms or molecules at emitting sites on the cathode. Such fluctuations appear as a square-wave modulation of the predischarge field emission current. In addition, these experiments have positively verified that the condition of the anode may play a significant role in introducing additional major fluctuations in current. Associated with this second type of fluctuation was the proliferation of small whisker-like projections on both electrodes. The above fluctuations in current could be greatly reduced only by previously cleaning both electrodes by thermal heating.

The proliferation of small whiskers under contaminated conditions has been ascertained only in a limited number of experimental observations. Further studies of this phenomenon are currently under way.

REFERENCES

1. D. Skaperdas and H. Knoebel, "Final Report, Coordinated Science Laboratory Electric Vacuum Gyro," CSL Report R-195, February 1964.

2. E. M. Lyman, D. A. Lee, H. E. Tomaschke and D. Alpert, "The Effect of Gas Pressure on Electrical Breakdown and Field Emission," Proceedings of Second International Symposium on Insulation of High Voltages in Vacuum," 7-8 September 1966. pp. 33-40.

3. D. Alpert, D. A. Lee, E. M. Lyman and H. E. Tomaschke, "The Effect of Gas Pressure on Electrical Breakdown and Field Emission," to appear as a Communication in J. Appl. Phys. in 1967.

4. D. Alpert, D. A. Lee, E. M. Lyman and H. E. Tomaschke, J. Vac. Sci. Tech. 1, 35 (1964).

5. C. M. Turner, Phys. Rev. 81, (1951).

6. J. L. McKibben and K. Boyer, Phys. Rev. 82A, 315 (1951).

7. E. G. Linder and S. M. Christian, J. Appl. Phys. 23, 1213 (1952).

8. G. E. Vibrans, MIT Lincoln Laboratory Tech. Report 308 (1963), "Computation of the Spreading of an Electron Beam under Acceleration and Space-Charge Repulsion."

9. H. E. Tomaschke, University of Illinois Coordinated Science Laboratory Thesis, Report R-192 (1964), "A Study of the Projections on Electrodes and Their Effects on Electrical Breakdown in Vacuum."

10. R. D. Young and E. W. Müller, J. Appl. Phys. 33, 91 (1962).

11. H. E. Tomaschke, op. cit.

12. D. Alpert, D. A. Lee, H. E. Tomaschke and E. M. Lyman, op. cit., J. Vac. Sci. Tech.

13. I. Brodie, J. Vac. Sci. Tech. 3, 222 (1966).

14. Pavel Kranjec and Lawrence Ruby, "A Test of the Critical-Field Theory of Electrical Breakdown in Vacuum," to be published in March-April 1967 issue of J. Vac. Sci. Tech.

15. D. Alpert, D. A. Lee, E. M. Lyman and H. E. Tomaschke, op. cit., J. Vac. Sci. Tech.

16. W. S. Boyle, P. Kisliuk and L. H. Germer, J. Appl. Phys. 26, 720 (1955).

17. I. Brodie, J. Appl. Phys. 35, 2324 (1964).

18. R. A. Millikan and C. C. Lauritsen, Proc. Nat. Acad. Sci. 14, 45 (1928).

19. R. P. Little and S. T. Smith, J. Appl. Phys. 36, 1502 (1965).

20. I. Brodie and I. Weissman, Vacuum 14, 299 (1964).

21. B. Singer and H. D. Doolittle, J. Appl. Phys. 36, 2002 (1965).

22. R. E. Burgess, H. Kroemer and J. M. Houston, Phys. Rev. 90, 515 (1953).

23. D. Alpert, D. A. Lee, E. M. Lyman and H. E. Tomaschke, op. cit., J. Vac. Sci. Tech.

24. W. S. Boyle, P. Kisliuk and L. H. Germer, op. cit.

25. R. P. Little and S. T. Smith, op. cit.

26. I. Brodie and I. Weissman, op. cit.

27. H. E. Tomaschke, op. cit.

28. W. P. Dyke and J. K. Trolan, Phys. Rev. 89, 799 (1953).

29. W. P. Dyke, J. K. Trolan, E. E. Martin and J. P. Barbour, Phys. Rev. 91, 1043 (1953).

30. W. W. Dolan, W. P. Dyke and J. K. Trolan, Phys. Rev. 91, 1054 (1953)

31. H. C. Miller and G. A. Farrall, J. Appl. Phys. 36, 1338 (1965).

32. I. Brodie, op. cit., J. Appl. Phys.

33. L. I. Pivovar and V. I. Gordienko, Soviet Phys. - Tech. Phys. 7, 908 (1963).

34. P. A. Redhead, Vacuum 13, 253 (1963).

35. R. A. Millikan and C. C. Lauritsen, op. cit.

36. H. Tomaschke and D. Alpert, J. Appl. Phys. (to be published).

37. I. Brodie, J. Vac. Sci. Tech. 2, 249 (1965).

Distribution list as of May 1, 1966

1 Dr. Edward M. Reilley
Asst. Director (Research)
Ofc. of Defense Res. & Engrg.
Department of Defense
Washington, D. C. 20301

1 Office of Deputy Director
(Research and Information Rm 3D1037)
Department of Defense
The Pentagon
Washington, D. C. 20301

1 Director
Advanced Research Projects Agency
Department of Defense
Washington, D. C. 20301

1 Director for Materials Sciences
Advanced Research Projects Agency
Department of Defense
Washington, D. C. 20301

1 Headquarters
Defense Communications Agency (333)
The Pentagon
Washington, D. C. 20305

20 Defense Documentation Center
Attn: TISIA
Cameron Station, Building 5
Alexandria, Virginia 22314

1 Director
National Security Agency
Attn: Librarian C-332
Fort George G. Meade, Maryland 20755

1 Weapons Systems Evaluation Group
Attn: Col. Finis G. Johnson
Department of Defense
Washington, D. C. 20305

1 National Security Agency
Attn: R4-James Tippet
Office of Research
Fort George G. Meade, Maryland 20755

1 Central Intelligence Agency
Attn: OCR/DD Publications
Washington, D. C. 20505

1 AFRSTE
Hqs. USAF
Room 1D-429, The Pentagon
Washington, D. C. 20330

1 AUL3T-9663
Maxwell Air Force Base, Alabama 36112

1 AFFTC (FTBPP-2)
Technical Library
Edwards AFB, California 93523

1 Space Systems Division
Air Force Systems Command
Los Angeles Air Force Station
Los Angeles, California 90045
Attn: SSSD

1 SSD(SSTRT/Lt. Starbuck)
AFUPO
Los Angeles, California 90045

1 Det. #6, OAR (LOOAR)
Air Force Unit Post Office
Los Angeles, California 90045

1 Systems Engineering Group (RTD)
Technical Information Reference Branch
Attn. SEPIR
Directorate of Engineering Standards
& Technical Information
Wright-Patterson AFB, Ohio 45433

1 ARL (ARIY)
Wright-Patterson AFB, Ohio 45433

1 AFAL (AVT)
Wright-Patterson AFB, Ohio 45433

1 AFAL (AVTE/R. D. Larson)
Wright-Patterson AFB, Ohio 45433

1 Office of Research Analyses
Attn: Technical Library Branch
Holloman AFB, New Mexico 88330

2 Commanding General
Attn: STEWS-WS-VT
White Sands Missile Range
New Mexico 88002

1 RADC (EMLAL-1)
Griffiss AFB, New York 13442
Attn: Documents Library

1 Academy Library (DFSLB)
U. S. Air Force Academy
Colorado 80840

1 FJSRL
USAF Academy, Colorado 80840

1 APGC (PGRPS-12)
Eglin AFB, Florida 32542

1 AFETR Technical Library
(ETV, MU-135)
Patrick AFB, Florida 32925

1 AFETR (ETLLG-1)
STINFO Officer (for Library)
Patrick AFB, Florida 32925

1 AFCRL (CRMXLR)
AFCRL Research Library, Stop 29
L. G. Hanscom Field
Bedford, Massachusetts 01731

2 ESD (ESTI)
L. G. Hanscom Field
Bedford, Massachusetts 01731

1 AEDC (ARO, INC)
Attn: Library/Documents
Arnold AFS, Tennessee 37389

2 European Office of Aerospace Research
Shell Building
47 Rue Cantersteen
Brussels, Belgium

5 Lt. Col. E. P. Gaines, Jr.
Chief, Electronics Division
Directorate of Engineering Sciences
Air Force Office of Scientific Research
Washington, D. C. 20333

1 U. S. Army Research Office
Attn. Physical Sciences Division
3045 Columbia Pike
Arlington, Virginia 22204

1 Research Plans Office
U. S. Army Research Office
3045 Columbia Pike
Arlington, Virginia 22204

1 Commanding General
U. S. Army Materiel Command
Attn: AMCRD-RS-PE-E
Washington, D. C. 20315

1 Commanding General
U. S. Army Strategic Communications Command
Washington, D. C. 20315

1 Commanding Officer
U. S. Army Materials Research Agency
Watertown Arsenal
Watertown, Massachusetts 02172

1 Commanding Officer
U. S. Army Ballistics Research Laboratory
Attn: V. W. Richards
Aberdeen Proving Ground
Aberdeen, Maryland 21005

1 Commandant
U. S. Army Air Defense School
Attn: Missile Sciences Division C&S Dept.
P. O. Box 9390
Fort Bliss, Texas 79916

1 Commanding General
U. S. Army Missile Command
Attn: Technical Library
Redstone Arsenal, Alabama 35809

1 Commanding General
Frankford Arsenal
Attn: SMUFA-L6000 (Dr. Sidney Ross)
Philadelphia, Pennsylvania 19137

1 U. S. Army Munitions Command
Attn: Technical Information Branch
Picatinney Arsenal
Dover, New Jersey 07801

1 Commanding Officer
Harry Diamond Laboratories
Attn: Mr. Berthold Altman
Connecticut Avenue & Van Ness Street N. W.
Washington, D. C. 20438

1 Commanding Officer
U. S. Army Security Agency
Arlington Hall
Arlington, Virginia 22212

1 Commanding Officer
U. S. Army Limited War Laboratory
Attn: Technical Director
Aberdeen Proving Ground
Aberdeen, Maryland 21005

1 Commanding Officer
Human Engineering Laboratories
Aberdeen Proving Ground, Maryland 21005

1 Director
U. S. Army Engineer Geodesy, Intelligence
and Mapping
Research and Development Agency
Fort Belvoir, Virginia 22060

1 Commandant
U. S. Army Command and General Staff College
Attn: Secretary
Fort Leavenworth, Kansas 66270

1 Dr. H. Robl, Deputy Chief Scientist
U. S. Army Research Office (Durham)
Box CM, Duke Station
Durham, North Carolina 27706

1 Commanding Officer
U. S. Army Research Office (Durham)
Attn: CRD-AA-IP (Richard O. Ulsh)
Box CM, Duke Station
Durham, North Carolina 27706

1 Superintendent
U. S. Army Military Academy
West Point, New York 10996

1 The Walter Reed Institute of Research
Walter Reed Medical Center
Washington, D. C. 20012

1 Commanding Officer
U. S. Army Electronics R&D Activity
Fort Huachuca, Arizona 85163

1 Commanding Officer
U. S. Army Engineer R&D Laboratory
Attn: STINFO Branch
Fort Belvoir, Virginia 22060

1 Commanding Officer
U. S. Army Electronics R&D Activity
White Sands Missile Range, New Mexico 88002

1 Dr. S. Benedict Levin, Director
Institute for Exploratory Research
U. S. Army Electronics Command
Fort Monmouth, New Jersey 07703

1 Director
Institute for Exploratory Research
U. S. Army Electronics Command
Attn: Mr. Robert O. Parker, Executive
Secretary, JSTAC (AMSEL-XL-D)
Fort Monmouth, New Jersey 07703

1 Commanding General
U. S. Army Electronics Command
Fort Monmouth, New Jersey 07703

Attn: AMSEL-SC
RD-D
RD-C
RD-GF
RD-MAF-I
RD-MAT
XL-D
XL-E
XL-C
XL-S
HL-D
HL-L
HL-J
HL-P
HL-O
HL-R
NL-D
NL-A
NL-P
NL-R
NL-S
KL-D
KL-E
KL-S
KL-T
VL-D
WL-D

3 Chief of Naval Research
Department of the Navy
Washington, D. C. 20360
Attn: Code 427

4 Chief, Bureau of Ships
Department of the Navy
Washington, D. C. 20360

3 Chief, Bureau of Weapons
Department of the Navy
Washington, D. C. 20360

2 Commanding Officer
Office of Naval Research Branch Office
Box 39, Navy No. 100 F.P.O.
New York, New York 09510

3 Commanding Officer
Office of Naval Research Branch Office
219 South Dearborn Street
Chicago, Illinois 60604

1 Commanding Officer
Office of Naval Research Branch Office
1030 East Green Street
Pasadena, California

1 Commanding Officer
Office of Naval Research Branch Office
207 West 24th Street
New York, New York 10011

Distribution list as of May 1, 1966 (cont'd.)

1 Commanding Officer
Office of Naval Research Branch Office
495 Summer Street
Boston, Massachusetts 02210

8 Director, Naval Research Laboratory
Technical Information Officer
Washington, D. C.
Attn: Code 2000

1 Commander
Naval Air Development and Material Center
Johnsville, Pennsylvania 18974

2 Librarian
U. S. Naval Electronics Laboratory
San Diego, California 95152

1 Commanding Officer and Director
U. S. Naval Underwater Sound Laboratory
Fort Trumbull
New London, Connecticut 06840

1 Librarian
U. S. Navy Post Graduate School
Monterey, California

1 Commander
U. S. Naval Air Missile Test Center
Point Magu, California

1 Director
U. S. Naval Observatory
Washington, D. C.

2 Chief of Naval Operations
OP-07
Washington, D. C.

1 Director, U. S. Naval Security Group
Attn: G43
3801 Nebraska Avenue
Washington, D. C.

2 Commanding Officer
Naval Ordnance Laboratory
White Oak, Maryland

1 Commanding Officer
Naval Ordnance Laboratory
Corona, California

1 Commanding Officer
Naval Ordnance Test Station
China Lake, California

1 Commanding Officer
Naval Avionics Facility
Indianapolis, Indiana

1 Commanding Officer
Naval Training Device Center
Orlando, Florida

1 U. S. Naval Weapons Laboratory
Dahlgren, Virginia

1 Weapons Systems Test Division
Naval Air Test Center
Patuxtent River, Maryland
Attn: Library

1 Mr. Charles F. Yost
Special Assistant to the Director of Research
National Aeronautics and Space Administration
Washington, D. C. 20546

1 Dr. H. Harrison, Code RRE
Chief, Electrophysics Branch
National Aeronautics and Space Administration
Washington, D. C. 20546

1 Goddard Space Flight Center
National Aeronautics and Space Administration
Attn: Library, Documents Section Code 252
Greenbelt, Maryland 20771

1 NASA Lewis Research Center
Attn: Library
21000 Brookpark Road
Cleveland, Ohio 44135

1 National Science Foundation
Attn: Dr. John R. Lehmann
Division of Engineering
1800 G Street, N. W.
Washington, D. C. 20550

1 U. S. Atomic Energy Commission
Division of Technical Information Extension
P. O. Box 62
Oak Ridge, Tennessee 37831

1 Los Alamos Scientific Laboratory
Attn: Reports Library
P. O. Box 1663
Los Alamos, New Mexico 87544

2 NASA Scientific & Technical Information Facility
Attn: Acquisitions Branch (S/AK/DL)
P. O. Box 33
College Park, Maryland 20740

1 Director
Research Laboratory of Electronics
Massachusetts Institute of Technology
Cambridge, Massachusetts 02139

1 Polytechnic Institute of Brooklyn
55 Johnson Street
Brooklyn, New York 11201
Attn: Mr. Jerome Fox
Research Coordinator

1 Director
Columbia Radiation Laboratory
Columbia University
538 West 120th Street
New York, New York 10027

1 Director
Coordinated Science Laboratory
University of Illinois
Urbana, Illinois 61801

1 Director
Stanford Electronics Laboratories
Stanford University
Stanford, California

1 Director
Electronics Research Laboratory
University of California
Berkeley 4, California

1 Director
Electronic Sciences Laboratory
University of Southern California
Los Angeles, California 90007

1 Professor A. A. Dougal, Director
Laboratories for Electronics and
Related Sciences Research
University of Texas
Austin, Texas 78712

1 Division of Engineering and Applied Physics
210 Pierce Hall
Harvard University
Cambridge, Massachusetts 02138

1 Aerospace Corporation
P. O. Box 95085
Los Angeles, California 90045
Attn: Library Acquisitions Group

1 Professor Nicholas George
California Institute of Technology
Pasadena, California

1 Aeronautics Library
Graduate Aeronautical Laboratories
California Institute of Technology
1201 E. California Boulevard
Pasadena, California 91109

1 Director, USAF Project RAND
Via: Air Force Liaison Office
The RAND Corporation
1700 Main Street
Santa Monica, California 90406
Attn: Library

1 The Johns Hopkins University
Applied Physics Laboratory
8621 Georgia Avenue
Silver Spring, Maryland
Attn: Boris W. Kuvshinoff
Document Librarian

1 Hunt Library
Carnegie Institute of Technology
Schenley Park
Pittsburgh, Pennsylvania 15213

1 Dr. Leo Young
Stanford Research Institute
Menlo Park, California

1 Mr. Henry L. Bachmann
Assistant Chief Engineer
Wheeler Laboratories
122 Cuttermill Road
Great Neck, New York

1 University of Liege
Electronic Department
Mathmatics Institute
15, Avenue Des Tilleuls
Val-Benoit, Liege
Belgium

1 School of Engineering Sciences
Arizona State University
Tempe, Arizona

1 University of California at Los Angeles
Department of Engineering
Los Angeles, California

1 California Institute of Technology
Pasadena, California
Attn: Documents Library

1 University of California
Santa Barbara, California
Attn: Library

1 Carnegie Institute of Technology
Electrical Engineering Department
Pittsburgh, Pennsylvania

1 University of Michigan
Electrical Engineering Department
Ann Arbor, Michigan

1 New York University
College of Engineering
New York, New York

1 Syracuse University
Department of Electrical Engineering
Syracuse, New York

1 Yale University
Engineering Department
New Haven, Connecticut

1 Airborne Instruments Laboratory
Deerpark, New York

1 Bendix Pacific Division
11600 Sherman Way
North Hollywood, California

1 General Electric Company
Research Laboratories
Schenectady, New York

1 Lockheed Aircraft Corporation
P. O. Box 504
Sunnyvale, California

1 Raytheon Company
Bedford, Massachusetts
Attn: Librarian

Security Classification

DOCUMENT CONTROL DATA R&D

(Security classification of title, body of abstract and indexing annotation must be entered when the overall report is classified)

1. ORIGINATING ACTIVITY (Corporate author)
University of Illinois
Coordinated Science Laboratory
Urbana, Illinois 61801

2a. REPORT SECURITY CLASSIFICATION
Unclassified

2b. GROUP

3. REPORT TITLE
FINAL REPORT: STUDIES RELEVANT TO THE ELECTRIC VACUUM GYRO PROGRAM OF ELECTRICAL BREAKDOWN IN ULTRAHIGH VACUUM

4. DESCRIPTIVE NOTES (Type of report and inclusive dates)

5. AUTHOR(S) (Last name, first name, initial)
Lyman, Ernest M.

6. REPORT DATE
January, 1967

7a TOTAL NO. OF PAGES
61

7b. NO. OF REFS.
37

8a. CONTRACT OR GRANT NO.
DA 28 043 AMC 00073(E)

b. PROJECT NO.
20014501B31F; Also in part NGR 14 005 038

c.

d.

9a. ORIGINATOR'S REPORT NUMBER(S)
R-334

9b. OTHER REPORT NO(S) (Any other numbers that may be assigned this report)

10. AVAILABILITY/LIMITATION NOTICES
Distribution of this report is unlimited.

11. SUPPLEMENTARY NOTES

12. SPONSORING MILITARY ACTIVITY
Joint Services Electronics Program
thru U.S. Army Electronics Command
Ft. Monmouth, New Jersey 07703

13. ABSTRACT

This is the final report, submitted in fulfillment of the requirements of NASA Grant NGR 005 038 (terminated on 30 September 1966) and the Joint Services Electronics Program (U.S. Army, U.S. Navy, and U.S. Air Force) under Contract No. DA 28 043 AMC 0073(E).

Matters concerned with various aspects of the electrostatically levitated gyroscope have previously been reported in detail. The recent activities reported here have been concerned with a study of the nature of electrical breakdown in ultrahigh vacuum, and some measurements directly related to the gyro developement.

DD FORM 1 JAN 64 1473

Security Classification